INVESTIGATION OF CO_2-PHILIC OLIGOMERS FOR CARBON DIOXIDE/HYDROGEN MEMBRANE SEPARATIONS

by

Mary Katharine Barillas

BS in Chemical Engineering, Lafayette College, 2004

MS in Chemical Engineering, University of Pittsburgh, 2007

Submitted to the Graduate Faculty of

Swanson School of Engineering in partial fulfillment

of the requirements for the degree of

Doctor of Philosophy

University of Pittsburgh

2011

UNIVERSITY OF PITTSBURGH

SWANSON SCHOOL OF ENGINEERING

This dissertation was presented

by

Mary Katharine Barillas

It was defended on

April 4th, 2011

and approved by

David Luebke, PhD, National Energy Technology Laboratory

Sachin Velankar, PhD, Associate Professor, Department of Chemical and Petroleum Engineering

William Federspiel, PhD, W.K. Whiteford Professor, Department of Bioengineering/ Department of Chemical and Petroleum Engineering

Dissertation Director: Robert Enick, PhD, Bayer Professor, Department of Chemical and Petroleum Engineering

INVESTIGATION OF CO_2-PHILIC OLIGOMERS

FOR CARBON DIOXIDE/HYDROGEN MEMBRANE SEPARATIONS

Mary Katharine Barillas, PhD

University of Pittsburgh, 2011

The objective of this work was to design polymeric membranes that have very high CO_2 permeability and high mixed gas selectivity toward CO_2 rather than hydrogen. Therefore the membranes were based on "CO_2-philic" polymers that exhibit thermodynamically favorable Lewis acid:Lewis base and hydrogen bonding interactions with CO_2.

CO_2-philic polymers that are solid at ambient temperature include polyfluoroacrylate (PFA); polyvinyl acetate (PVAc); and amorphous polylactic acid (PLA). Literature CO_2 permeability values for PVAc and PLA are disappointingly low and are H_2 selective. The cast PFA membranes from this study had low permeabilities (45 barrers at 25 ^oC) and very low CO_2/H_2 selectivity of 1.4.

CO_2-philic polymers that are liquid at ambient conditions include polyethylene glycol (PEG), polypropylene glycol (PPG), polybutylene glycol with a linear -$((CH_2)_4O)$- repeat unit (i.e. polytetramethylene ether glycol (PTMEG)), polybutylene glycol (PBG) with a branched repeat unit, perfluoropolyether (PFPE), poly(dimethyl siloxane) (PDMS), and polyacetoxy oxetane (PAO). A small compound, glycerol triacetate (GTA) was also considered because it is commercially available and similar in chemical structure to a trimer of PVAc (small oligoimers of vinyl acetate are very difficult to synthesize). These liquids were tested as supported liquid membranes (SLM) and also (with the exception of PAO and GTA) as rubbery, crosslinked materials. Mixed gas permeability was measured using equimolar mixtures of CO_2 and H_2 feed

streams at one atmosphere total pressure in steady-state flux experiments over the 298 - 423 K temperature range.

The most promising SLMs were those composed of a PEG, PTMEG, GTA, and PDMS. For example, at 37 ^{o}C the PEG-, PTMEG-, GTA- and PDMS-based SLMs exhibited CO_2/H_2 selectivity values of ~ 11, 9, 9, and 3.5, respectively, and CO_2 permeability values of ~800, 900, 1900, and 2000 barrers, respectively. Crosslinked versions of the PEG, PTMEG and PDMS membranes at 37 ^{o}C exhibited selectivity values of ~ 5, 6 and 3.5, respectively, and CO_2 permeability values of ~50, 300, and 3000 barrers, respectively.

TABLE OF CONTENTS

LIST OF TABLES

LIST OF FIGURES

LIST OF SYMBOLS

Symbol	Description	Units
n	flux	$\left[\frac{\text{mol}}{\text{m}^2\text{s}}\right]$
P	permeability	$\left[\frac{\text{kmol m}}{\text{m}^2\text{s Pa}}\right]$
P	pressure	[Pa]
t_m	membrane thickness	[m]
$\alpha_{A/B}$	selectivity ratio	[-]
D	diffusion coefficient	$\left[\frac{\text{m}^2}{\text{s}}\right]$
S	solubility coefficient	$\left[\frac{\text{mol}}{\text{Pa m}^3}\right]$
v_o	occupied volume	$\left[\frac{\text{cm}^3}{\text{g}}\right]$
v	specific volume of polymer	$\left[\frac{\text{cm}^3}{\text{g}}\right]$
TGA	thermogravimetric analysis	
GC	gas chromatograph	
NMR	nuclear magnetic resonance	
SLM	supported liquid membrane	

XLM	crosslinked membrane
PEGDME	poly(ethylene glycol) dimethyl ether
PPGDME	poly(propylene glycol) dimethyl ether
PTMEGDAc	poly(trimethylene glycol) diacetate
PBGDAc	poly(butylene glycol) diacetate
PDMS	poly(dimethyl siloxane)
PFPE	perfluoropolyether
GTA	glycerol triacetate
PAO	poly(acetoxy oxetane)
PEGDA	poly(ethylene glycol) diacrylate
PPGDA	poly(propylene glycol) diacrylate
PBGDA	poly(butylene glycol) diacrylate
PTMEGDA	poly(trimethylene glycol) diacrylate

ACKNOWLEDGEMENTS

I would foremost like to thank my advisor Dr. Robert Enick for his support, his constant enthusiasm, his patience, and most importantly, the knowledge that I have gained. It has been very enjoyable working for an advisor with such a good attitude, who is always positive even if things go wrong and pushes you to your fullest potential. I also thank all Dr. David Luebke, Dr. Dr. Deepak Tapriyal, Christina Myers, Shan Wickramanayake and Dr. Bret Howard for providing me with guidance and helpful insight into my work.

I would also like to thank the members of my group: Deepak Tapriyal, James McClendon, Matt Miller, Dazun Xing, Hussein Baled and Bing Wei, for their helpful discussions and for generally making the lab an enjoyable place to work. Also, I thank the members of the Sequestration group at NETL Pittsburgh, especially Dr. Sheila Hedges for her assistance on the TGA and TGA/MS.

I gratefully acknowledge DuPont and Dow, for raw materials used in experiments, Bayer for supplying the acetylated poly(tetramethylene glyol) diacetate and the poly(butylene glycol) diacetate, and GE Global Research for the synthesis of poly(acetoxy oxetane).

Finally, I would like to thank my family, my friends, and my loving husband Jeff for their unconditional love and support along the way and helping to make me who I am today. Without their encouragement and understanding it would have been difficult to realize my dreams.

1.0 INTRODUCTION

Producing energy affordably, efficiently, and in an environmentally friendly manner is the key to keeping industrial processes viable. Several processes produce CO_2 (e.g. coal gasification) as a byproduct and a capture system must be developed that will either recycle or sequester the gas. There are several commercially viable ways of capturing CO_2, which include absorption, adsorption, cryogenic distillation, and membrane separation. Of these processes, CO_2 selective membranes could play an integral part of producing clean and efficient energy in systems requiring the separation of high pressure gas mixtures (e.g. coal gasification, natural gas production).

The capture of CO_2 from advanced power generation sources, such as the Integrated Gasification Combined Cycle (IGCC), and its subsequent geologic sequestration will increase the cost of power generation from these higher efficiency plants. However, improvements related to the selective removal CO_2 from a post-water gas shift reactor stream rich in CO_2, H_2 and water could reduce these expenses. The two most common separation techniques being considered for the CO_2/H_2 separation are physical absorption with solvents and membrane-based separation. The attributes of membrane-based separation units include mechanical simplicity, relatively low energy requirements, and a single-step separation mechanism with no need for regeneration. Some of the disadvantages of membranes include large material cost for high

throughput applications, fouling, limited commercial development, difficulty in attaining high product purity, and the limited thermal and chemical stability of many polymers.

Ideally, membranes would be able to maintain their mechanical integrity and favorable permeability and selectivity characteristics at the temperature of the water-gas shift reactor effluent, which is roughly 250 ^{o}C. The crosslinked polymers used in this study; however, would be viable only at temperatures less than 200 ^{o}C, the temperature at which conventional crosslinking groups become unstable. The supported liquid membranes could slowly volatilize at elevated temperatures or be displaced from the porous support if high differential pressures are applied across the membrane, and CO_2-philic solid polymer membranes typically have melting point values less than 100^{o}C. For strong size selective (glassy polymers) separations permeability increases as temperature increases; however for rubbery polymers permeability and diffusivity can be temperature dependent [1, 2]. Therefore it is expected that the water-gas shift effluent stream would have to be cooled substantially for polymeric membranes to be viable for this CO_2-H_2 separation. (For this reason, these CO_2-philic membranes will be subsequently examined for the CO_2-N_2 post-combustion separation, which is inherently low temperature.)

In this study, only reverse selective membranes (i.e. ones in which the larger gas molecule, CO_2, has a greater mixed gas permeability than the smaller gas component, H_2) were considered. For a dense polymeric material to act as a reverse selective solution-diffusion membrane, where permeability is the product of solubility and diffusivity, the solubility of CO_2 in the polymer must be so great that it more than compensates for the high hydrogen diffusivity in the polymer.

Membranes used for commercial gas separation processes are generally fabricated in the form of hollow fibers or rolled sheets. The types of membranes used in this lab-scale study,

however, include thin cast or thermally pressed films of amorphous polymers, supported liquid polymer membranes (SLM) retained in a porous Nylon fabric, or crosslinked polymeric films.

The films cast from a solvent of thermally pressed are composed of highly CO_2-philic solid polymers. Although this type of membrane is not used industrially, it is a convenient method for assessing the performance of membranes composed of the most CO_2-philic polymers that have ever been identified, which are the low melting point, amorphous solids such as poly(fluoroacrylate).

Although SLMs are easy to prepare and serve as excellent vehicles for quickly comparing the permeability and selectivity of polymers of oligomers, the slight vapor pressure of these liquids can compromise the integrity of the membrane placed in contact with flowing gases for extended periods of time. (Ionic liquids, rather than polymers or oligomers, may be more appropriate for long-term supported liquid membrane use because these molten salts exert no detectable vapor pressure.)

The flexible, crosslinked polymers (which are based on the same polymers used in the SLMs) are more practical membranes in that they are non-volatile and have excellent mechanical properties.

1.1 IGCC

IGCC is a process that needs efficient CO_2 separations to be viable. The IGCC process is essentially the combination of the gasification and combustion process at one location. Coal is gasified to form synthesis gas (syngas) of CO and H_2. The gas then undergoes the water–gas shift, in which CO reacts with steam to form CO_2 and H_2. The CO_2 is must be removed, and the

H_2 is sent to a gas turbine combined cycle. This particular coal technology has been indicated as CO_2 capture ready for carbon dioxide sequestration. CO_2-selective membranes could be an integral part of the process to transform coal into hydrogen fuel while capturing CO_2 for sequestration.

One alternative to this separation process is oxyfuel combustion. This eliminates the production of NO_x because the fuel is combusted with pure oxygen instead of air. In this process the CO_2 can easily be separated; however the development of materials that can withstand the temperature achieved by oxyfuel combustion is still a problem [3, 4].

There are several locations where membranes can be utilized in the IGCC process. These include immediately after a low temperature water gas shift (WGS) or after the gases have been cooled and finally at the CO_2 compressor inter-stage. Initially the polymers are being developed for the post WGS CO_2 capture, also known as "pre-combustion" capture. The conditions that exist at each of these locations are listed in Table 1. The flow chart in Figure 1 depicts a simplified, but typical IGCC plant. As we move left to right the ease of integrating a membrane is increased however the driving force for membranes integration decreases.

Table 1. Preferred membrane operating temperatures: IGCC Applications [5]

	Membrane Location	Temperature, ˚C	Pressure, psia
1	After cold-gas clean-up	40-100	300-650
2	Post low-T water gas shift (after warm gas cleanup)	100-450	300-650
3	CO_2 compressor interstage	40	50-100

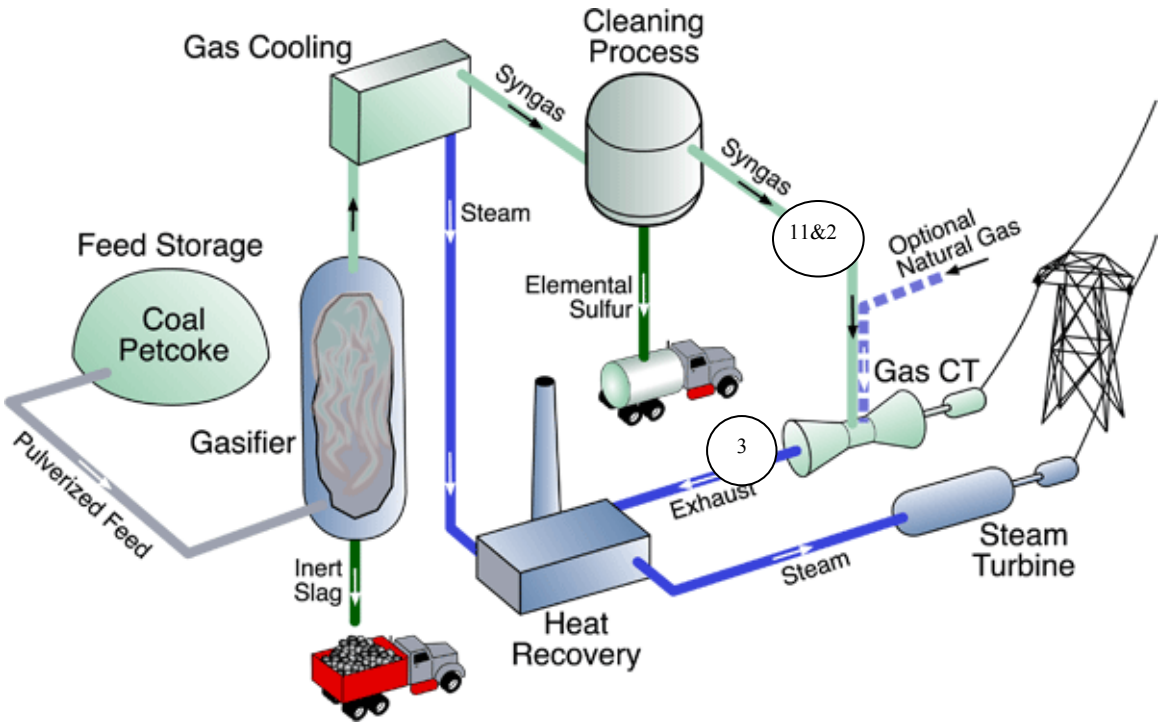

Figure 1. Simplified IGCC flow diagram and possible membrane integration [6]

The DOE has proposed some program goals for capture carbon capture and sequestration from IGCC processes. These include the pre-combustion capture of 90% or greater from future IGCC plants and an increase of the cost of electricity (COE) of 10% or less. From these requirements for the IGCC process simulations were performed by Ciferno and Marano to establish the necessary selectivity required for membranes at the 2006/2007 baseline COE for CO_2 capture on an IGCC plant. Based on these process simulations it is necessary to create a membrane with a H_2/CO_2 selectivity of at least 40 and membrane cost less than \$0.40/GPU-cm^2*10^3 [GPU = gas permeation unit] to have definite potential where it exceeds performance of a state of the art IGCC with carbon capture[7].

These CO_2 selective membranes could also be used for another important gas mixture; CO_2/CH_4. This mixture is associated with the production of methane that contains an undesirable

acid gas such as CO2. The membrane would function in a "sweetening" mode during gas processing as a passive apparatus for the removal of (no heating value) CO_2. It could also be used for post-combustion capture flue gas mixtures of CO_2/N_2; however, the low pressure gradient used in this separation would not be advantageous for our transport mechanism.

Numerous polymers have been previously tested for CO_2-separations. The proposed work is distinguished by the selection and design of polymers that display particularly high solubility in supercritical or liquid CO_2.

1.2 CARBON CAPTURE TECHNOLOGIES

Currently there are several methods for capturing CO_2 from several industrial processes. These processes are summarized along with the advantages and disadvantages of using these processes in Table 2 [8].

Table 2. Carbon Capture Techniques

CO_2 Separation Technique	Example	Advantages	Disadvantages
Chemical Absorption (typically low P)	Monoethanolamine (MEA)	Commercially mature process	Large equipment sizes and high-regeneration energy requirements
Physical Absorption (typically high P)	Selexsol (PEGDME), Rectisol (Chilled Methanol)	Commercially mature process	Less energy-intensive than the MEA process
Alkaline Salt	Aqueous solutions of sodium and potassium carbonate	Low cost and minimal degradation	Slow reaction rate Large heating requirement Foaming
Cryogenic Distillation	Liquefy and separate	Good economies of scale	Need a relatively pure source (>90% CO2) High energy requirement
Solid physical adsorption	Pressure swing Temperature swing (eg. zeolites)	"Easy" to handle and that they do not give rise to corrosion problems	Can require long regeneration cycles
Membranes	Polysep(UOP)- PRISM (Monsanto, Air Products and Chemicals).	Small footprint, Mechanical, simplicity, High energy efficiency No regeneration, Compact, Lightweight, Passive	Cannot attain extremely high purities Low temperature/chemical stability

1.3 PERMEATION THROUGH POLYMER MEMBRANES

There are five main types of advanced membrane technologies: polymer, metal, silica, zeolite, and carbon [9] which each have a method of gas transport. The methods of gas transport are Poiseuille flow, Knudsen diffusion, molecular sieving, capillary condensation, surface diffusion and solution diffusion. The particular type of membrane that this research will focus on is polymeric membranes. The polymer membranes generally function on the idea that either the gases are separated based on their size or solubility in the polymers. Transport of materials through dense polymeric membranes occurs through solution diffusion. The gases initially sorb into the polymer matrix, then diffuse through the micropores (polymer matrix), and then desorb on the other side of the membrane. Transport of gases occurs through Fick's First Law shown in Equation 1.

$$n = -D\nabla C \qquad 1$$

where n is the diffusive flux, D is the diffusion coefficient, C is the local concentration. If we look at one dimensional non-bulk flow is the equation for flux becomes Equation 2.

$$n_a = -D\frac{\partial C}{\partial x} \qquad 2$$

The integrated form of this equation is shown in Equation 3.

$$n = \frac{C_2 - C_1}{t_m} D \qquad 3$$

where n, is the flux through the membrane, $C_{2,}$ is the upstream(retentate) concentration, $C_{1,}$ is the downstream (permeate) concentration, D, is the diffusivity coefficient and t_m is the thickness of the membrane. This is illustrated in Figure 2.

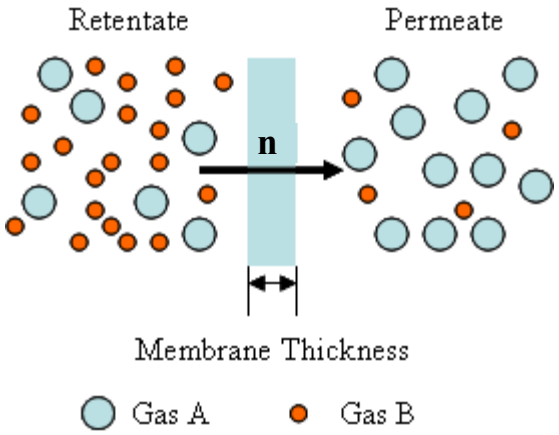

Figure 2. Flux through dense polymeric membrane

The permeability of gases can be expressed as (Equation 4):

$$P = \frac{n\, t_m}{p_2 - p_1} \qquad 4$$

where P is permeability, n is flux of gas, t_m is thickness, p_2 is the partial pressure of the gas in the retentate, and p_1 is the partial pressure of the gas in the permeate.

In the case of dense rubbery polymer materials, penetrant concentration, p, is related to the solubility according to Henry's law where the equilibrium concentration is defined by Equation 5.

$$C_i = S_i p_i \qquad 5$$

where S_i is the sorption coefficient, p_i is external partial pressure, and C_i is the equilibrium concentration of the gas in the polymer (generally less than 10% by volume) [1].

By substituting the definition of flux into the permeability in Equation 4, the relationship of permeability to solubility can be seen in Equation 6.

$$P = \frac{n\, t_m}{p_2 - p_1} = \frac{C_2 - C_1}{p_2 - p_1} D \qquad 6$$

In our study the concentrations of the gases in the permeate will be very low compared to the concentration in the retentate and therefore Equation 6 becomes:

$$P = \frac{C_2}{p_2} D \quad \textbf{or} \quad P = S_2 D \qquad 7$$

The permeability of a non-porous polymeric membrane is the product of the diffusivity and solubility of the gas, P = DS. The selectivity (α) of a pair of gases is simply the ratio of their permeability and therefore also their diffusivity and solubility:

$$\alpha_{a/b} = \frac{P_a}{P_b} = \frac{D_a}{D_b}\frac{S_a}{S_b} \qquad 8$$

There are two ways to define selectivity: ideal, which is based on the ratio of single gas permeability measurements, and permselectivity, which is based on mixed gas experiments. Generally these two values are nearly the same as long as there are not specific interactions between the gases; however, many times the permselectivity is lower than the ideal selectivity. In the case of poly(ethylene oxide) it has been shown that at temperatures of -20℃ the selectivity can actually increase due to polymeric swelling [10].

The diffusivity selectivity is based on size. For the separation of CO_2 from H_2 the size selectivity will always favor H_2 because the kinetic diameter of H_2 is smaller than CO_2 (see Table 3). The kinetic diameter is essentially the smallest diameter of a spacing needed to let that specific molecule pass.

The sorption capability of a gas is generally a function of the condensability of the component to be separated as well as the affinity of the gas for the polymer; the higher the condensability the higher the sorption capability. Based on the critical temperature of the two gases to be studied the CO_2 is more condensable and therefore the solubility selectivity will be greater than unity for CO_2. This is the fundamental reason that the separation of CO_2 and H_2 with

membranes is so challenging; H_2 is smaller and can diffuse more easily than CO_2, but CO_2 is more condensable and therefore typically displays higher solubility in the polymer. Glassy polymers ($T_{operating}<T_g$) are generally those which separate based on the size of the gas molecules, whereas rubbery polymers ($T_{operating}>T_g$) separate based on enhanced transport due to the high solubility of the gas in the polymer[11, 12].

Table 3. Size and Condensability of H_2 and CO_2

	Size	**Condensability**
Gas	**Kinetic diameter (Å)**	**Critical Temperature (K)**
H_2	**2.89**	**33.2**
CO_2	**3.3**	**132.9**

1.3.1 Fractional Free Volume

Fractional free volume (FFV) gives an estimate of the amount of space between chains available for gas permeation. It can be calculated using Equation 9:

$$FFV = \frac{v - v_o}{v} \qquad 9$$

where v, is the specific volume (the molecular weight of the polymer divided by the density $\left[\frac{M_w}{\rho}\right]$ and v_o, is the molar volume of the polymer. Bondi suggest the use of group contribution to identify the molar volume (v_o) from the van der Waals volume (v_w) using:

$$v_o = 1.3 \times v_w \quad (10)$$

Combining Equation 9 and Equation 10 yields an equation that contains measureable parameters.

$$FFV = 1 - \frac{1.3 \times \rho \times v_w}{M_w} \quad (11)$$

The use of FFV comes into play for the calculation of diffusivity and permeability in particular. The diffusivity of the polymer is related to the free volume by Equation 12.

$$D = Ae^{\frac{-B}{FFV}} \quad (12)$$

where A and B are empirical constants which depend on penetrant size and polymer and FFV is the fractional free volume.

Permeability has a very similar relationship for FFV and is expressed in Equation 13.

$$D = Ae^{\frac{-B}{FFV}} \quad (13)$$

1.3.2 Temperature Dependence on Permeation

The temperature dependence of permeability, diffusivity and solubility can be expressed as Arrehenius relationships. The relationship for permeability is defined as:

$$P = P_o e^{\frac{-E_p}{RT}} \quad (14)$$

Where P_o, is the pre-exponential for permeability, E_p, is the activation energy for permeation, R, is the universal gas constant and T, is the temperature.

The relationship for diffusion is defined as:

$$D = D_o e^{\frac{-Ed}{RT}} \quad (15)$$

Where D_o, is the pre-exponential for permeability, E_d, is the activation energy for diffusion of the amount of energy required to move a gas molecule from one open space in the polymer to another, R, is the universal gas constant and T, is the temperature.

The relationship for solubility is defined as:

$$S = S_o e^{\frac{-H_s}{RT}} \qquad 16$$

Where S_o, is the pre-exponential for solubility, H_s, is the heat of sorption, R, is the universal gas constant and T, is the temperature.

1.4 SEPARATION OF CO_2 AND H_2

The membrane separation of CO_2 and H_2 has two options: hydrogen selective and reverse selective or CO_2-selective. Numerous polymers have been tested for this particular separation and the "Robeson plot" trade-off or relationship between selectivity and permeability for H_2-selective membranes is shown in Figure 3 [13]. This is a compilation of all data collected to date and includes ideal and permselective data at various temperatures and pressures. The curve is an empirical relationship, which has been set with the uppermost data.

First we must decide whether or not we want to have hydrogen selective or reverse selective (CO_2 selective) membranes. Because our group has identified several polymers, which have a chemical affinity for CO_2, reverse selective polymers will be examined. When applying these polymers to this separation, the retentate side will be maintained at a high pressure whereas the CO_2 will permeate through the membrane and produce a lower pressure stream which can then be recycled to produce chemicals [14] or can be sequestered.

For our experiments we will use a sweep gas; however, there is a possibility of this sweep gas permeating into the retentate and in commercial use an additional separation is necessary if the sweep gas cannot be co-sequestered or used. The high pressure retentate is composed of H_2, which can be used as an energy source.

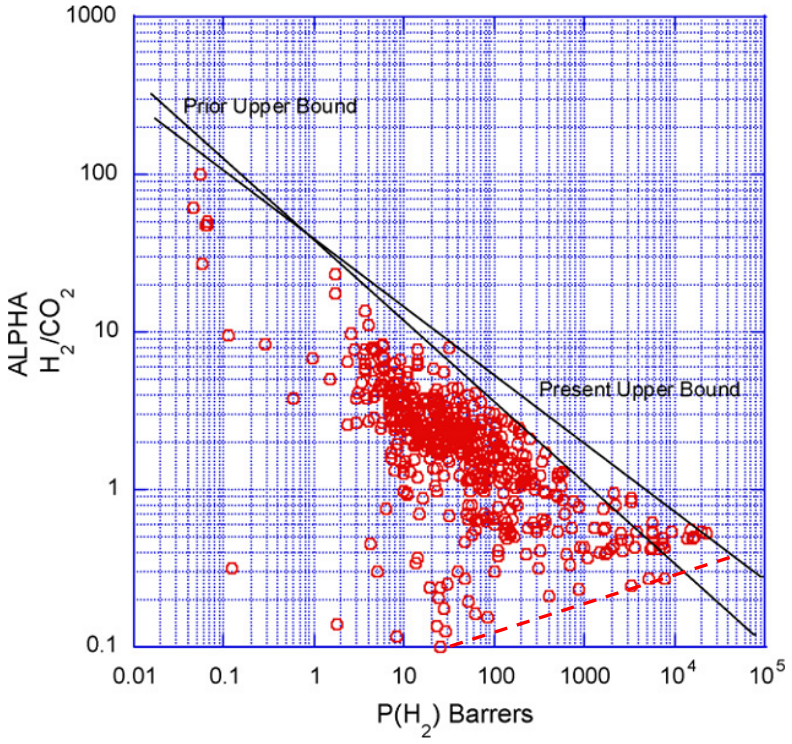

Figure 3. The trade-off of permeability and selectivity for the gas pair H_2/CO_2. Graph shows the H_2 permeability vs selectivity (H_2/CO_2) for a range of pressures and temperatures as well as the upperbound[13]. Reprinted from Journal of Membrane Science, 320/1-2, Lloyd M. Robeson, The upper bound revisited, 390-400., Copyright 2008, with permission from Elsevier

The literature plot shown in Figure 3 illustrate that selectivity values for CO_2 over H_2 in a CO_2-selective membrane generally do not exceed a value of 10. This plot also indicates an upperbound for H_2 selective membranes; however it will be discussed in the future work section that there may be an upperbound for CO_2 selective membranes (dashed line; not a Robeson bound) that should have a negative slope indicating a tradeoff between permeability and selectivity. Further, CO_2 permeability values associated with CO_2/H_2 selectivity values of at least 5 rarely exceed 2000 barrers. (A barrer=$1\times10^{-10}\,\frac{\mathrm{cm}^3(\mathrm{STP})\,\mathrm{cm}}{\mathrm{cm}^2\,\mathrm{s}\,\mathrm{cmHg}}$. Extremely high permeability values (~18000 barrers) are possible, but the CO_2/H_2 selectivity drops to a value of about 2. The dashed line, which has been drawn as a potential upper-limit for the CO_2 upper bound for CO_2-selective (reverse-selective) membranes, indicates that, unless a material breakthrough is attained, attaining a selectivity of 40 will only be achieved with CO_2 permeability values as low as 1 barrer. According to Franz and Sherer to attain membranes that satisfy the requirements of CO_2 separation degrees of 85% with a purity of 95% and a efficiency loss below 10% points, membranes have to achieve a selectivity of 150 for a single stage membrane or with a cascade concept the selectivity has to be 60, assuming a permeability of $(9.41\times10-13)\times10-5\left[\frac{\mathrm{kmol}}{\mathrm{s\ Pa\ m}}\right]$ or 28.1 barrers [15]. For a H_2 selective membrane a H_2/CO_2 selectivity of 50 and permeability of $(2.61\times10-13)\times10-5\left[\frac{\mathrm{kmol}}{\mathrm{s\ Pa\ m}}\right]$ or 7.8 barrers can achieve the same goal. [15]

1.5 DESIGNING POLYMERS FOR CO_2/H_2 SEPARATION

In general the first things to consider when choosing a polymer as a membrane material are its physical properties such as chemical resistance, mechanical strength and the ability to process the polymer into a useful form. Secondly, to make CO_2 selective membranes, there are several characteristics that have been found to produce CO_2 selective membranes and include:

1. High fractional free volume (PTMSP, PDMS, etc)
    a. Fractional free volume indicates the amount of free space per unit volume that is available for intramolecular motion. This intramolecular rearrangement of molecular segments to allow gases to diffuse through polymer matrix; higher intramolecular motion means that gases can diffuse through the polymer more easily.
    b. Since diffusion is a function of the minimum free volume; the higher free volume the higher the diffusion coefficient, but if the free volume is too high, diffusion selectivity will dominate.
    c. Rubbery polymers exhibit high diffusivities since there is more ability of the chains to rearrange to incorporate the diffusing gases.
    d. One of the highest free volumes found in a polymer is polyacetylenes (namely poly(trimethylsilyl propene) (PTMSP) whose free volume fraction is 20-25% [16]; however this polymer is actually quite rigid and the chain structure allows for a "microporosity" which allows gases to exhibit higher permeabilities.
2. Polarity
    a. Need to have specific sites for favorable polymer-CO_2 interactions, which promote CO_2 solubility in the polymer. (e.g. Lewis acid-Lewis base [17, 18])

1.6 CO_2-PHILIC POLYMER DESIGN

What makes a polymer CO_2-philic? As described in this dissertation, it will be a polymer which can dissolve in dilute concentrations (e.g. 5wt%) into CO_2 at extremely high pressures and has very specific thermodynamic interactions with CO_2. These polymers generally have the following characteristics [19]:

1. Acetylation generally leads to CO_2 solubility; however, it does not ensure it.
2. Amorphous, flexible chains and high free volume (note: this property has also been shown to lead to high permeability membranes)
3. Previous research has shown branching increases the free volume of the solute thereby decreasing the intramolecular interactions between polymer segments.
4. Oxygen rich: ether groups, carbonyls, acetates (every highly CO_2 soluble polymer is oxygenated). Some of the best CO_2 selective polymers contain ether groups and are highly selective [11])
5. Amine functional groups should be avoided (to increase the H_2 permeability, the opposite would be true). Amine functional groups generally lead to complexation (eg. carbamates, carbamic acid)[20].
6. Methylene spacers between the polymer backbone and acetate groups should be avoided. This has been demonstrated empirically, but the reason for it has not been ascertained.

Figure 4 is a plot of the cloud point of several polymers that will be tested as polymeric membranes. The cloud point is measured at 5 wt% polymer in CO_2 and establishes the pressure at which the polymer and the CO_2 form a single phase (below this pressure two phases exist). The 5 wt% concentration is commonly used in these comparisons because a maximum in the P_x cloud point locus typically occurs at a concentration near 5 wt%. These cloud points are a very

good indicator of the polymer/solvent interaction. The lower the cloud point the better the CO_2 acts as a solvent to the polymer. The perfluoropolyacrylate PHDFDA has shown the lowest cloud point with CO_2 to date.

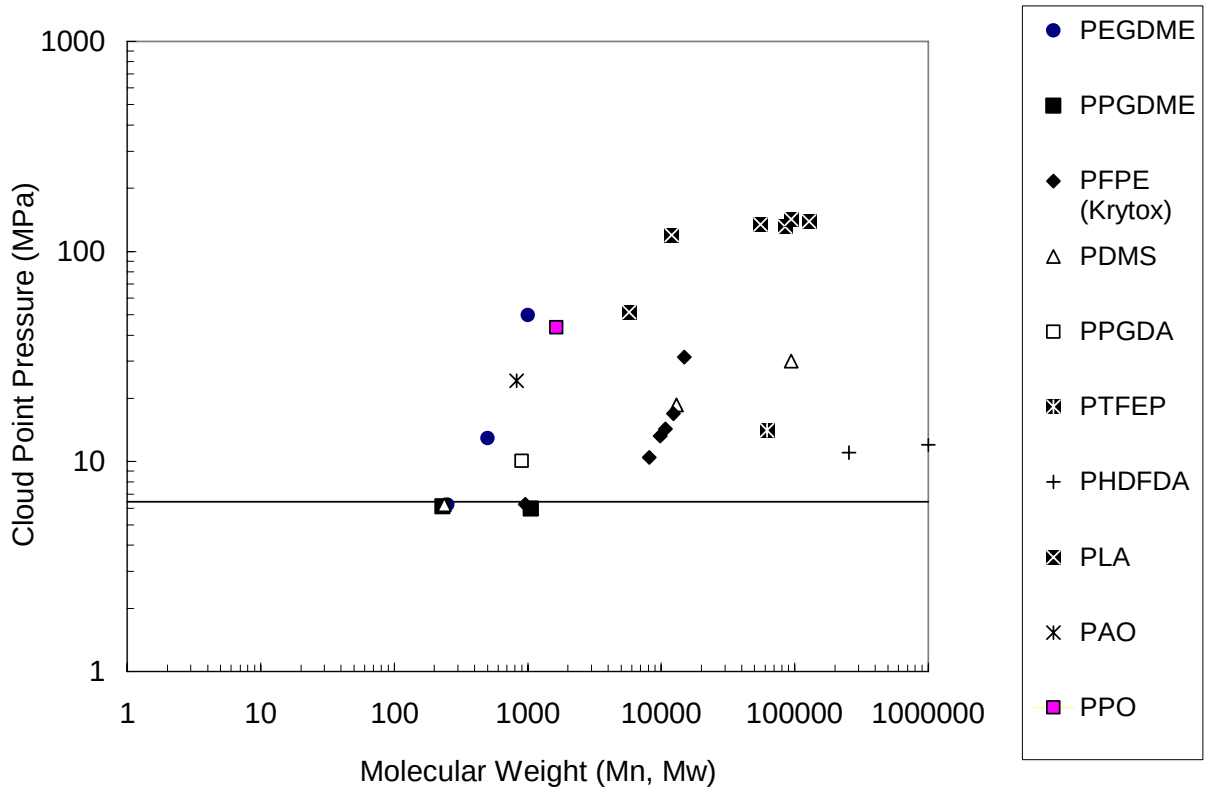

Figure 4. Two phase pressure at 5wt% polymer in CO_2 for several polymers [21-25]

1.7 PREVIOUSLY TESTED POLYMERS FOR CO_2/H_2 SEPARATION

Polymers that have been previously assessed for removing CO_2 from a mixed gas CO_2/H_2 stream include polyphosphazenes, PEO-based materials, polymers with ultra-high free volume and fluoropolymers [10, 11, 26-38]. Polyphosphazenes were able to achieve CO_2 permeability of 250 barrers with a CO_2/H_2 selectivity of 10 at 30 ˚C [27]. Amorphous PEO had a CO_2 permeability

of 140 barrers and a CO_2/H_2 of 6.8 at 35 ˚C [11]. Pure PEO has a tendency to crystallize at higher molecular weights, which greatly diminishes its permeability. PEG-containing copolymers of polyurethanes, polyimides and polyamides exhibited separation factors as high as ~7 [31]. PEBAX, a polyether-block-amide, has been studied as a CO_2 membrane material and as the matrix of a semi-interpenetrating membrane in conjunction with a CO_2-philic, PEG-based, liquid oligomer [32]. Pure PEBAX has shown a permeability of 73 barrers and a selectivity of 9.1 at 30 ˚C[37]. A 50:50 (wt%) PEBAX -poly(ethylene glycol) dimethyl ether (PEGDME) semi-interpenetrating network membranes had a CO_2 permeability of 606 barrers and a CO_2/H_2 selectivity to 15.2 at 30 ˚C[37]. Ultra-high free volume polymers generally yield highly permeable membranes (e.g. up to ~44000 barrers) but the selectivity of CO_2/H_2 is ~2[38]. For most ultra-high free volume polymers the permeability order is $CO_2 > H_2 > He > O_2 > Ar > CH_4 > N_2 > Xe$[39]. From the references mentioned here only one of the studies included mixed gas results[10], the rest of the results were performed using single gas permeation techniques, whereas this research is primarily focused on mixed gas permeability and selectivity.

1.8 RESEARCH OBJECTIVES/SPECIFIC AIMS

The polymers chosen for this work have been previously shown to be highly "CO_2-philic" in that they are capable of dissolving in CO_2 at concentrations of ~5 wt% at extremely high pressure (1000-10000 psi), and/or they have been shown to be excellent solvents for the absorption of CO_2 [40-42]. The partial pressure of CO_2 in an IGCC plant is expected to be only several hundred psia, well below the pressure required for the polymer to dissolve in CO_2. The representative temperature and pressure after the low tempature water gas shift are 200-320□C

and 300-600 psia [ref marano]; therefore there is no danger of these CO_2-philic membranes dissolving during the gas separation, particularly the crosslinked materials. These polymers include: poly(heptadecafluorodecyl acrylate), a polyfluoroacrylate (PFA), probably the most CO_2-philic polymer that has been identified to date; polyvinyl acetate (PVAc), the most CO_2-philic oxygenated hydrocarbon-based polymer; amorphous polylactic acid (PLA); poly-3-acetoxy oxetane (PAO), a highly acetylated polymer designed via molecular modeling that exhibits a large number of multi-point interactions with CO_2; perfluoropolyether (PFPE), a polyhexafluoropropylene oxide Krytox® oil; polydimethyl siloxane (PDMS), commonly referred to as silicone oil; polyethyleneglycol dimethylether (PEGDME), a major constituent of the Selexol® CO_2 solvent; polypropyleneglycol dimethylether (PPGDME), which has a branched monomeric unit; polybutyleneglycol diacetate that is based on a linear -($(CH_2)_4O$)- monomeric unit, also known as poly(tetramethylene ether glycol) diacetate (PTMEGDAc), and polybutyleneglycol diacetate (PBGDAc) with a branched monomeric unit. A small compound, glycerol triacetate (GTA) was also selected for study as a supported liquid membrane because its structure is analogous to a trimer of PVAc (it is very difficult to synthesize low viscosity oligomers of vinyl acetate). The primary mechanism responsible for the remarkable levels of solubility in CO_2 are the multiple-point Lewis acid:Lewis base interactions and weak hydrogen bonding interactions between CO_2 and the backbone and side-chains of the polymers [40-42].

It is our contention that because these polymers have such favorable thermodynamic interactions with CO_2, they are excellent candidates for forming CO_2-permeable and CO_2-selective membranes. Specifically, it is expected that these favorable interactions between CO_2 and the polymer will enhance the solubility of the CO_2 in the polymer dramatically, thereby enhancing the CO_2 permeability and selectivity.

The only solid polymer used in this study, PFA, was knife cast into a dense film. This was the only manner in which this extremely fragile membrane, with a low melting point (~71 ^{o}C, measured by DSC) polymer could be made with enough mechanical integrity to be mounted and sealed into the membrane holder without tearing or cracking.

The liquid polymers, PFPE, PDMS, PEGDME, PPGDME, PTMEGDAc, PBGDAc and PAO, and the small compound GTA were first tested as SLMs. Our intent in studying the supported liquid membranes was not primarily to propose such membranes for commercial application, where the high total pressure drop across the membrane and the appreciable vapor pressure of the oligomers would render them impractical for extended use. Rather, it was recognized to be a simple means of preparing a membrane that could be used to quickly assess the polymer's CO_2 permeability. Crosslinking typically diminishes CO_2 permeability because the crosslinking functionalities are less CO_2-philic than the polymeric segments and because of the "blockage" of free volume caused by cross-linked network, therefore it was expected that the SLM permeability values would exceed those of the corresponding crosslinked membranes.

PFPE, PDMS, PEG, PPG, PTMEG, and PBG were crosslinked in order to be assessed as rubbery, flexible films that serve as more robust membranes. PAO and GTA could not be end-functionalized for crosslinking, however.

Our results, along with prior literature results for CO_2-selective polymeric membranes, will be presented on a plot of mixed gas CO_2/H_2 selectivity vs. CO_2 permeability, facilitating the identification of the polymers that exhibit relatively high mixed gas CO_2 selectivity and permeability.

1. Measure the transport properties at ambient conditions as well as elevated temperatures to investigate the performance of linear and branched polyethers (C2-C4) for CO_2 pre-combustion capture
2. Measure the transport properties at ambient conditions as well as elevated temperatures to investigate the performance of higly oxygenated CO_2-philic oligomers for CO_2 pre-combustion capture
3. Measure the transport properties at ambient conditions as well as elevated temperatures to investigate the performance of PEGDME for CO_2 pre-combustion capture with H_2S

2.0 MATERIALS

Several polymer candidates have been chosen for use as supported liquid membranes to be used in the constant pressure apparatus. These polymers are both liquid and solids (polyethers are likely to be liquids; polyfluoroacrylates are solids). The liquids are capable of being tested as supported liquids or, upon crosslinking, as flexible films; while the solids will be formed into dense films.

2.1 SUPPORTED LIQUID MATERIALS

Some important things to consider are the vapor pressures of the polymers, which will determine the upper limit of the use of these membranes. Since the transport mechanism is similar for supported liquid membranes as it is for dense polymer films the constant pressure membrane system will be used to analyze the permeability and selectivity of these supported liquid films.

There are several advantages of using the liquid polymers, such as the ease of preparation (does not require casting method). The membranes are produced by sorbing the liquid into the pores of a microporous support material. They also have higher permeabilities compared to the dense film membranes composed of the same polymer. There are several disadvantages to using supported liquid membranes, namely the evaporation of the supported liquids during long-term

exposure of the membrane to the retentate and permeate gas streams, and the displacement of the liquid from the membrane due to transmembrane pressure. Barrier materials are being designed to prevent evaporation of these supported liquids, but will not be the focus of this work. All the liquid polymers and oligomers used as supported liquid membranes in this study will also be cross-linked into dense flexible films to be used in the constant pressure apparatus. It should be expected that the permeability should decrease slightly due to the "blockage" of free volume caused by cross-linked network formed. This could enhance the selectivity because the diffusion coefficient of H_2 should decrease and the solubility selectivity could increase in CO_2. These films will also be tested at increased temperatures in the constant pressure apparatus.

2.1.1 Poly(ethylene glycol) dimethyl ether (PEGDME)

PEGDME was chosen because of the ether groups along the backbone of the polymer. A dimethyl ether endgroup was chosen because it would have a higher affinity to CO_2 compared with a diol endgroup. The PEGDME was obtained from Sigma Aldrich(Mn ~500 g/mol) and used as received. The structure is shown in Figure 5.

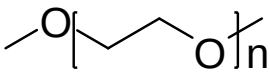

Figure 5. Structure of Poly(ethylene glycol) dimethyl ether

2.1.2 Poly(propylene glycol) dimethyl ether (PPGDME)

PPGDME was also chosen due to the ether groups along the backbone of the polymer. Again dimethyl ether endgroup was chosen because it would have a higher affinity to CO_2 compared with a diol endgroup. A branched backbone was chosen to examine the effect of adding a methyl group along the backbone to the permeability and selectivity. The methyl group should increase the fractional free volume and increase the permeability. The PPGDME was obtained from Polymer Source Inc. (MW~1060 g/mol) and used as received. The structure is shown in Figure 6.

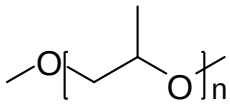

Figure 6. Structure of Poly(propylene glycol) dimethyl ether

2.1.3 Poly(butylene glycol) Diacetate (PBGDAc) and Poly(tetramethylene glycol) diacetate (PTMEGDAc)

PBGDAc and PTMEGDAc were chosen due to the ether groups along the backbone of the polymer. A diacetate endgroup was chosen because it would have a higher affinity to CO2 compared with a diol endgroup. A linear and branched version of PBGDAc were obtained in order to see the effect of using a longer linear ether as well as a longer ether with a methyl branch. The PBGDAc was obtained from Huntsman (MW~3000 g/mol) and PTMEGDAc was obtained from Bayer (MW~650 g/mol) and used as received. The structure of PBGDAc is shown in Figure 7. The structure of PTMEGDAc is shown in Figure 8.

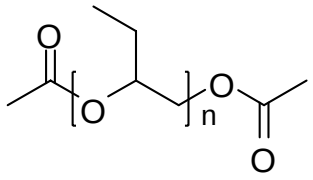

Figure 7. Structure of Poly(butylene glycol) diacetate (PBGDAc)

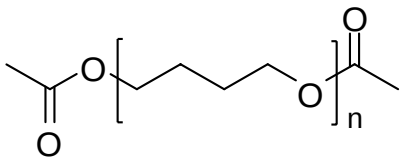

Figure 8. Structure of Poly(tetramethylene glycol) diacetate (PTMEGDAc)

2.1.4 Perfluoropolyether (PFPE)

Perfluoropolyether was chosen due to previous studies that demonstrate the solubility of these polymers in CO_2 [19]. The PFPE sold as Dupont Krytox oil was obtained from Miller Stephenson (Mn ~7475 g/mol and Mn~960 g/mol). By using two different molecular weights, the effect of molecular weight on permeability will be shown. The structure of PFPE is shown in Figure 9.

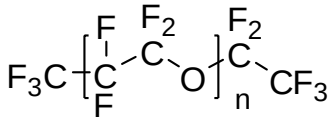

Figure 9. Structure of Perfluoropolyether (PFPE)

2.1.5 Polydimethyl siloxane (PDMS)

It has been suggested that the high solubility of CO_2 in poly (siloxanes) could be due to specific interactions between the oxygen atoms of CO_2 and Si atoms[18, 43]. The PDMS was obtained as a free sample from Dow Corning at two molecular weights (100cSt, Mn ~6000 g/mol and 5cSt, Mn~770 g/mol) to determine the effect of molecular weight on permeability. The structure of PDMS is shown in Figure 10.

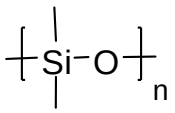

Figure 10. Structure of Polydimethyl siloxane (PDMS)

2.1.6 Glycerol triacetate (GTA)

Glycerol triacetate was chosen because it is highly oxygenated as well as it essentially a trimer of poly(vinyl acetate) (Figure 11a). Poly(vinyl acetate) has shown some of the highest CO_2 solubility with a polymer composed of C,H,O. Glycerol triacetate was obtained from Sigma Aldrich and used as received. The structure of glycerol triacetate is shown in Figure 11b.

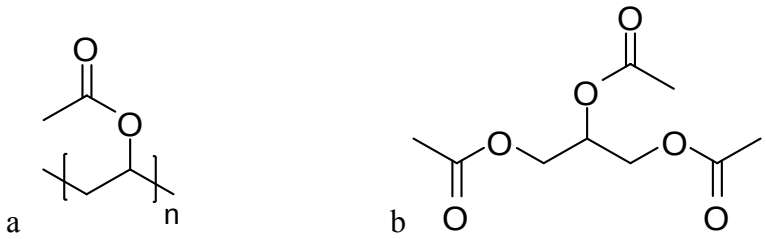

Figure 11. Structure of a)poly(vinyl acetate) and b)Glycerol Triacetate (GTA)

2.1.7 Poly(acetoxy oxetane) (PAO)

Poly (acetoxy oxetane) has shown some of the strongest interactions with CO_2 comprised solely of C, H and O, based on molecular modeling studies. GE Global synthesized this liquid oligomer in a form that will allow us to perform supported liquid membrane testing.

The materials required for the synthesis of PAO were used as received from SigmaAldrich. PAO was prepared by GE Global via the acetylation of polyglycidol. Polyglycidol was synthesized using a modification of the procedure of Sandler and Berg[44]. 10.0 g of glycidol was mixed with 100 mg of triethylamine and allowed to stir at room temperature for 2 days. The viscosity of the blend had increased substantially during this time. Proton NMR (DMDO-d6) showed there to be a small amount of epoxy remaining, therefore the mixture was heated at 40°C overnight. At this point the reaction mix was dissolved in 90 mL of methanol and treated with 2.4 g of Amberlite IR-120H. It was then filtered and the solvent was stripped off using a rotary evaporator. Toluene was then added and the mixture was re-stripped in order to remove any residual water, which would interfere with NMR analysis. The result was 9.69 g of viscous, yellow oil. The types of hydroxyls present were then measured using the NMR procedure of Vandenberg et. al.[45] , which indicated that the majority of the hydroxyls were from secondary alcohols and is consistent with branched oligomers. The branched polyglycidol oil was then mixed with 20 mL of acetic anhydride and heated 75-80°C. There were two phases observed at this time. 200 mg of 4-dimethylamino pyridine were then added, which caused the mixture to become homogenous. Heating was continued up to 90°C where the reaction was kept overnight. After cooling to room temperature the mix was diluted with water and extracted two times with chloroform. The combined organics were then washed with 10% sodium hydroxide followed by 10% HCl. After drying over anhydrous potassium carbonate, the

solution was filtered and stripped on a rotary evaporator to give 13.0 g of poly(3-acetoxy oxetane) product as a viscous yellow oil. The proton and ^{13}C NMRs confirmed the structure shown in Table 1. The molecular weight was estimated as 694 (n ~3) from end group analysis of the proton NMR results as shown in Appendix A.

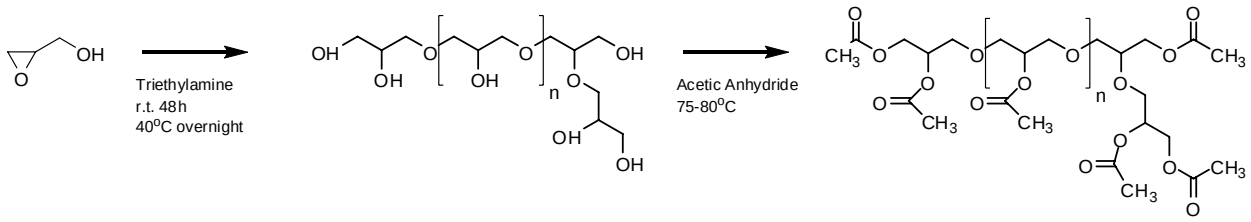

Figure 12. Procedure for PAO Synthesis

The material we were trying to obtain is shown in Figure 13(a) and what we obtained was a highly branched version which may cause some difference in the ability of this material to perform for permeability and selectivity.

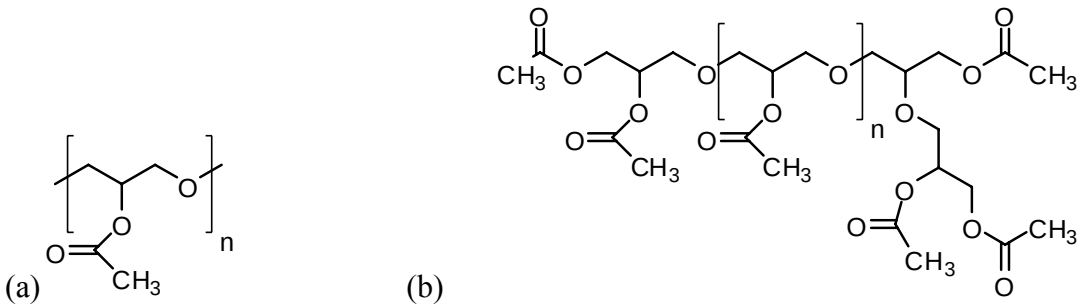

Figure 13. Structure of PAO (a) Backbone (b) Highly branched PAO

2.1.8 Support Material

The support material used in the preparation of SLMs was a porous nylon under the trade name Biodyne A (Pall Corporation) membrane and is an amphoteric Nylon 6,6. The important specifications for this material are shown in Table 4. The structure of nylon 6,6 is shown in Figure 14.

Table 4. Biodyne A: Support material specifications

Pore Size	0.2 μm
Diameter	1 inch
Typical thickness	152 μm (6.0 mils ± 0.5 mils)

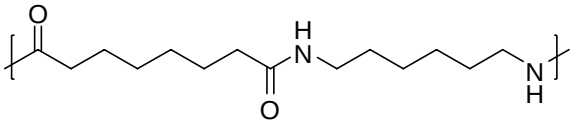

Figure 14. Structure of Biodyne A or Nylon 6,6

2.2 SOLID FILM MATERIALS

2.2.1 Poly(heptadecafluorodecyl acrylate)

The poly(HDFDA) polymer was chosen because it had the highest solubility in CO_2 compared to any other polymer. This polymer is semi-crystalline, which can lead to a decrease in the diffusivity. The synthesis is described in reference[46]. Poly(heptadecafluorodecyl acrylate) (PHDFDA) [which was to be knife cast into a dense membrane] was synthesized via solution polymerization from the monomer 3,3,4,4,5,5,6,6,7,7,8,8,9,9,10,10,10-heptadecafluorodecyl acrylate (≥90 % technical grade, Sigma Aldrich)[46]. For a typical experiment, 10 g of the heptadecafluorodecyl acrylate monomer and 5 mg of initiator (AIBN) were added into a 50-mL round bottom flask under N_2. Ten milliliters of trifluorotoluene was then added to the flask. The reaction was mixed at 333 K, yielding a transparent solution, and the polymerization was allowed to proceed for 24 h. The resultant polymer solution was then cooled to ambient temperature, removed from the flask, and washed three times with methanol. The PHDFDA precipitated out of solution. This perfluoroacrylate (PFA) was recovered by filtration, followed by overnight drying under vacuum, which produced a white powder with a yield of 80%. The synthesis and structure are shown in Figure 15.

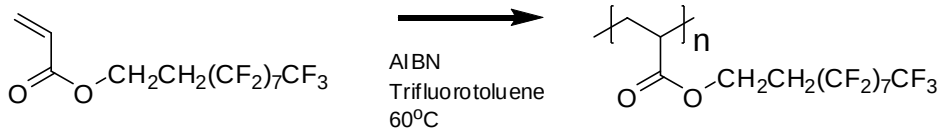

Figure 15. Synthesis of PHDFDA

2.2.2 PFPE-plasticized amorphous Teflon

Teflon AF has previously been shown to be extremely permeable membrane material and has high temperature stability, and is chemically resistant. Teflon AF 2400 has shown gas CO_2 and H_2 permeabilities of 2800 barrers and 2200 barrers respectively[47]. Teflon AF is a glassy polymer which has an extremely high free volume. The selectivity of Teflon AF has been shown to shift from size-selective to solubility-selective based on the degree of plasticization. We will test the shift in selectivity by using a perfluoropolyether plasticized Teflon AF. The PFPE that will be used to plasticize the Teflon AF will be the same as that used for the supported liquid membrane tests. The structure of the Teflon AF and the Krytox used are in Figure 16.

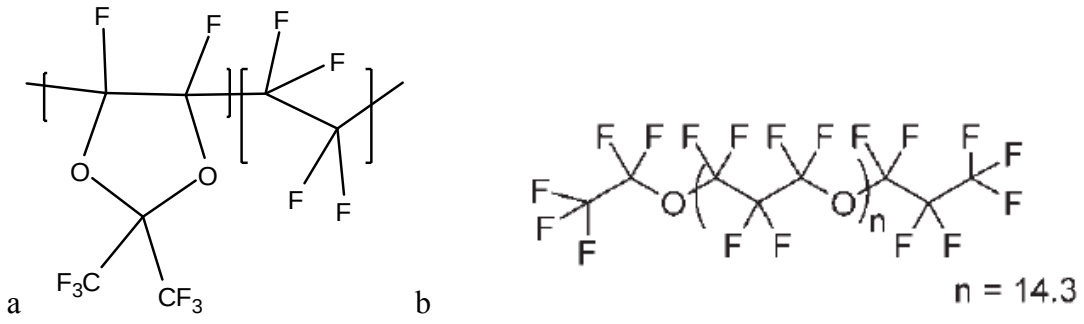

Figure 16. Structure of a)Teflon AF and b)Krytox

2.2.3 Crosslinked Membrane Materials

The following polymers were used in dense film study for the preparation of crosslinked membranes: polyethylene glycol diacrylate (PEGDA) (Sigma Aldrich, MW~700 g/mol), polypropylene glycol diacrylate (PPGDA) (Sigma Aldrich, Mn~900 g/mol), a crosslinkable PFPE (Shin Etsu Sifel 3400) based on perfluoropolyethylene oxide with siloxane reactive end groups, crosslinked PDMS (McMasterCarr, sheet 0.0005" thick), PTMEG diacrylate and PBG diacrylate. The poly(butylene glycol) diacrylate was produced from a poly(butylene glycol) diol with a linear monomeric repeat unit (Polysciences, MW~650, and Huntsman 3000 g/mol) through the procedure described in reference [48] and as shown in Figure 17.

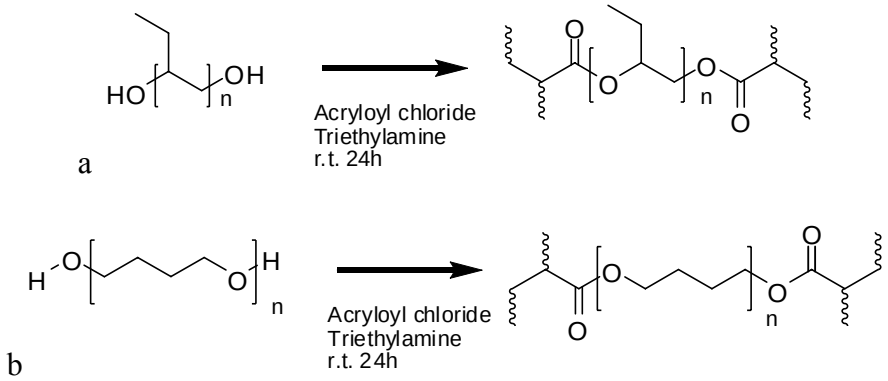

Figure 17. Synthesis of a) PBGDA and b)PTMEGDA

The PEGDA and PPGDA were passed through a prepacked inhibitor removal column purchased from Sigma Adlrich that removes the inhibitor 4-methoxyphenol (MEHQ) present in

the materials obtained; however, the column is not specifically recommended to remove the BHT also present in the starting material.

2.3 MEMBRANE PREPARATION

SLMs of PFPE, PDMS, PPGDME, PEGDME, PBGDAc, PTMEGDAc PAO, and GTA were produced by drop-coating the polymer onto the porous support and allowing diffusion of polymer into the nylon pores (pore diameter~0.2 μm) for ~3 hours. The membranes were then patted dry in order to remove excess polymer. The membranes were ~152 microns thick and had an active area of 2.2 cm^2. The thickness of the membrane was assumed to be the thickness of the fabric.

Solid films of PFA were prepared by solvent casting 20 wt% of PFA in the fluorinated solvent Vertrel XF. A 10 mil (1 mil= 2.54×10^{-5}m=0.001 in) casting knife was used to prepare the membrane. The mechanical stability of a free standing membrane film was difficult to achieve so a freestanding film was masked off using adhesive foil [49]. Using weight measurements, the polymer density, and the membrane diameter, the average thickness of the membrane was calculated to be 10 microns.

The polymer films were produced at The University of Minnesota by Phillippe Buhlman and Elizabeth Lugert [50]. A typical membrane formation started with a certain weight percent of plasticizer in this case Krytox and polymer (Teflon AF) and an adequate amount of Fluorinert (FC-72, perflourohexanes) to dissolve the compounds. The mixture was then sealed and stirred for 24hrs to ensure dissolution. Once the solutions were homogeneous the samples were poured into a glass ring on top of a sheet of Teflon and glass plate. The samples were dried for at least 4

days at ambient temperature to remove the perfluorohexanes. The dense film membranes based on PEGDA, PPGDA, PTMEG and PBGDA were produced by thermally crosslinking these liquid diacrylates. Initially the diacrylates were passed through a separation column to remove the inhibitor. A prepolymer solution of each acrylate containing 0.1wt% AIBN was prepared, then the nylon support was soaked with the prepolymer solution and crosslinked using a compression heater. The membrane thickness was controlled using an aluminum spacer between two aluminum sheets. The PEGDA, PPGDA, PTMEG and PBGDA were crosslinked at 80 ˚C and 2500 psi for one hour onto a porous support. These membranes were measured using a caliper (±1 micron) to determine the thickness of the membrane. The thickness of these membranes ranged from 150 to 170 microns.

PFPE was crosslinked according to the instructions provided by the supplier. The A and B components were mixed in a weight ratio of 103:100 respectively. The two components were thoroughly mixed in a glass beaker. The mixture was then degassed for 30 minutes under vacuum. PFPE was thermally crosslinked at 150 ˚C and 2500 psi for 10 minutes in the compression heater.

Crosslinked PDMS was used as received from the supplier. PAO and GTA were not readily end-functionalized with acrylates to promote crosslinking, therefore PAO and GTA were used only as a SLM.

3.0 MEMBRANE CHARACTERIZATION

Several techniques will be used to characterize the membranes in this study. The most important characterization in this study is the measurement of permeability of CO_2 and H_2. Initial measurements of permeability were obtained by measuring the transient flux of pure gases from a fixed volume apparatus through a membrane; however, it was found that this apparatus lacked the sensitivity and reproducibility to characterize the membranes. Subsequent steady-state measurements of permeability were based on the transport of mixed gases through the membrane because it gave a better indication of the permeability that would be realized in the separation of mixed gases. This mixed gas data was used to determine mixed gas selectivity, which is more accurate technique than ideal selectivity based on pure gas flux measurements because it accounts for mixed gas effects (e.g. the plasticization of a polymer with absorbed CO_2) that cannot be accounted for in pure gas tests. Only the most selective membranes will also be tested for CO_2 solubility via sorption measurements.

3.1 PERMEABILITY MEASUREMENTS

The CO_2 permeability and CO_2/H_2 mixed gas selectivity values of these SLMs, cast membranes and flexible crosslinked membranes were determined by measuring the steady-state flux of two

components in a mixed gas stream permeating through the membrane, as described in previous works [51, 52]

The standard used in judging the performance of a membrane is the permeability or permeance. The permeability (P_a) is permeance (flux) (n) normalized using the thickness (t_m) of the membrane see following equation.

$$\text{permeability}(P_a) = \frac{\text{permeance}(k)}{\text{membrane thickness}(t_m)} \qquad 17$$

There are two experimental techniques which are used to measure permeability and these include the constant volume and constant pressure methods. The constant volume method measures the pressure drop of the retentate as a function of time and can be used to measure diffusivity, solubility and permeability. This apparatus is best suited for pure gas permeability measurements.

The constant pressure method is based on measuring the steady state flux that is permeating through the membrane while keeping a constant pressure difference across the membrane. Equation 18 can be used to calculate the permeability in a constant pressure method apparatus.

$$P_a = \frac{n_a t_m}{\Delta p_a} \qquad 18$$

where P_a is the permeability of gas A, n_a is the diffusive flux of gas A through the membrane, t_m is the membrane thickness and Δp_a is the partial pressure difference of gas A across the membrane. The units of permeability are barrers and are defined as:

$$1\,\text{barrer} = 1\times10^{-10}\,\frac{\text{cm}^3\,(\text{STP})\,\text{cm}}{\text{cm}^2\,\text{s}\,\text{cmHg}}$$

Permeance is defined to be the gas flow rate through the material, per unit of area and per unit of pressure difference across the material. The standard unit for permeance is a gas permeation unit (GPU) which is defined as:

$$1\,\text{GPU} = 7.5005\,\text{x}\,10^{-16}\,\frac{\text{m}^3}{\text{m}^2\,\text{s}\,\text{Pa}}$$

The mixed gas selectivity values were measured, as opposed to ideal selectivity values. Mixed gas experiments leads to more realistic measures of membrane performance because the presence of the second component can alter the transport properties of the membranes. For example, CO_2/H_2 mixed gas selectivity values for CO_2-selective membranes are typically lower than the ideal selectivity because the CO_2 can plasticize the membrane, enabling the flux of H_2 to be greater than one would expect based on experiments conducted with pure H_2; however, it has been shown that for crosslinked ethylene oxide polymers [10] the mixed gas selectivity increased at -10°C, due to swelling.

Although it is possible to design polymer membranes that are H_2-selective [e.g. $\alpha(H_2/CO_2) = 100$], these membranes typically have very low permeability values (~ 0.01 – 0.1 barrer) for hydrogen. Although some membranes have shown almost infinite selectivity for hydrogen the permeance is extremely low for large industrial uses[13]. In this work, however, our goal is to design CO_2-selective membranes characterized by higher CO_2 permeability values (> 1 barrers) and high selectivity values (>10).

3.2 CONSTANT PRESSURE ANALYSIS

The constant pressure method is based on measuring the steady state flux of a mixed gas that is permeating through the membrane while keeping a constant partial pressure difference of each component across the membrane. The overall schematic of the apparatus is shown in (Figure 18) where the details are described elsewhere [51, 52]. A constant composition of mixed gas (20% CO_2, 20% H_2, balance Ar) is flowing on the retentate side of the membrane. In general the permeate side is kept at atmospheric pressure; however, an Ar sweep gas is used to keep the partial pressures of the permeating gases low (but detectable and accurate) on the retentate side of the membrane. The permeate and retentate gas compositions are measured by the GC which has two TCD detectors. The membrane holder (Figure 19) is contained in an oven in order to have temperature control. The specifications for the membrane holder are shown in Table 5. The steady state flux is related to the permeability using Equation 4.

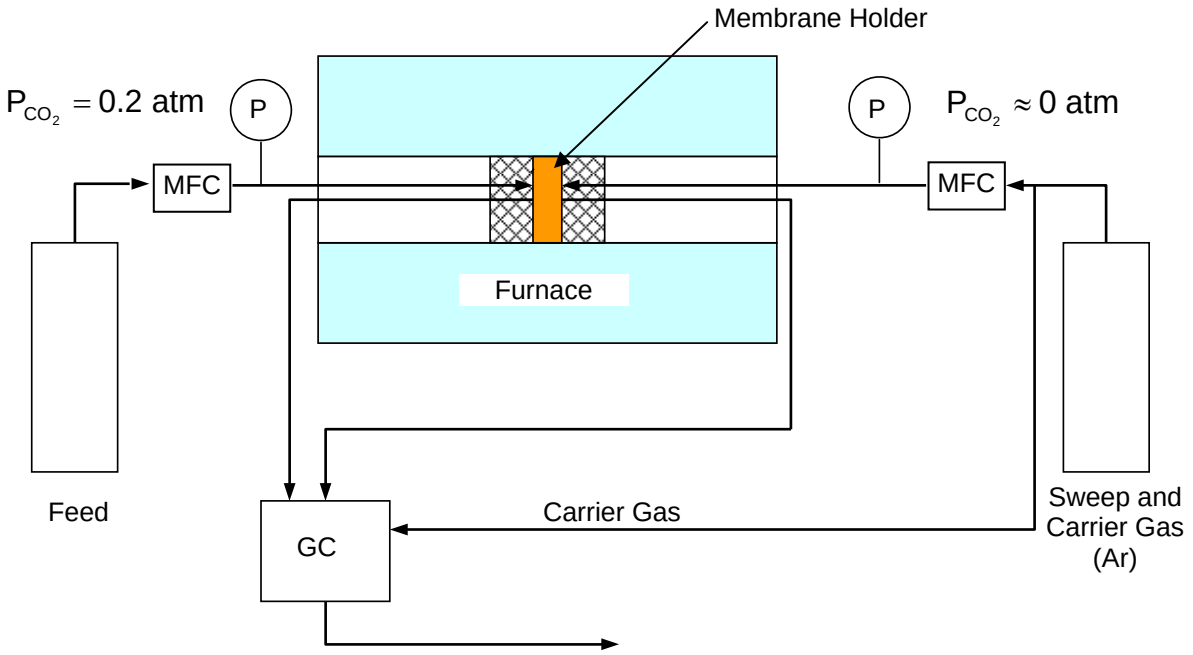

Figure 18. Schematic of experimental flow system used to measure the mixed gas permeability of the supported and dense film membranes in this study.

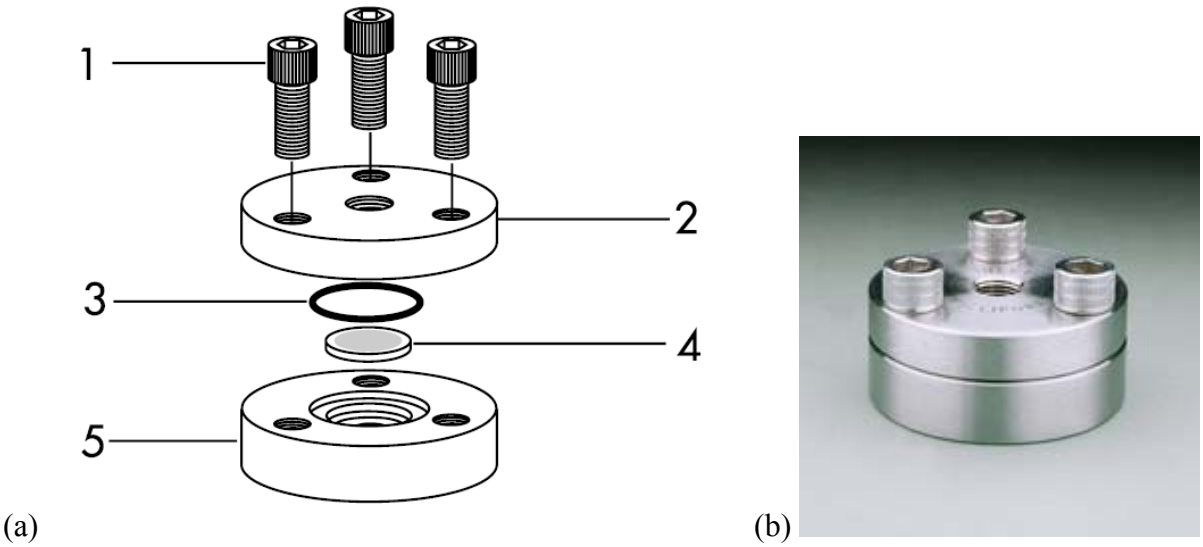

Figure 19. (a) Membrane holder blowup (1) Hex-cap screw (2) Inlet plate (3) O-ring (4) Filter screen (5) Outlet plate (b) Assembled membrane holder [53]

Table 5. Membrane Holder Specifications

Filter Diameter	25mm
Materials	316 Stainless steel holder; LCR-treated Buna-N resin O-ring
Filtration Area	2.2 cm^2
Differential Pressure Range	1000 psi for most filters

3.3 SORPTION

The sorption is measured using PCTPro-2000 from Setaram Instruments which uses the Sivert's method where the absorption is calculated from pressure change of a known volume. The temperature range of the system is ambient to 400^oC and the pressure range is vacuum to 200 bar. A sample at known pressure and volume is connected to a reservoir of known volume and pressure through an isolation valve. Opening the isolation valve allows new equilibrium to be established. Gas sorption is determined by difference in actual measured pressure (Pf) versus calculated pressure (Pc)[54]. The overall schematic of this system is shown in Figure 20.

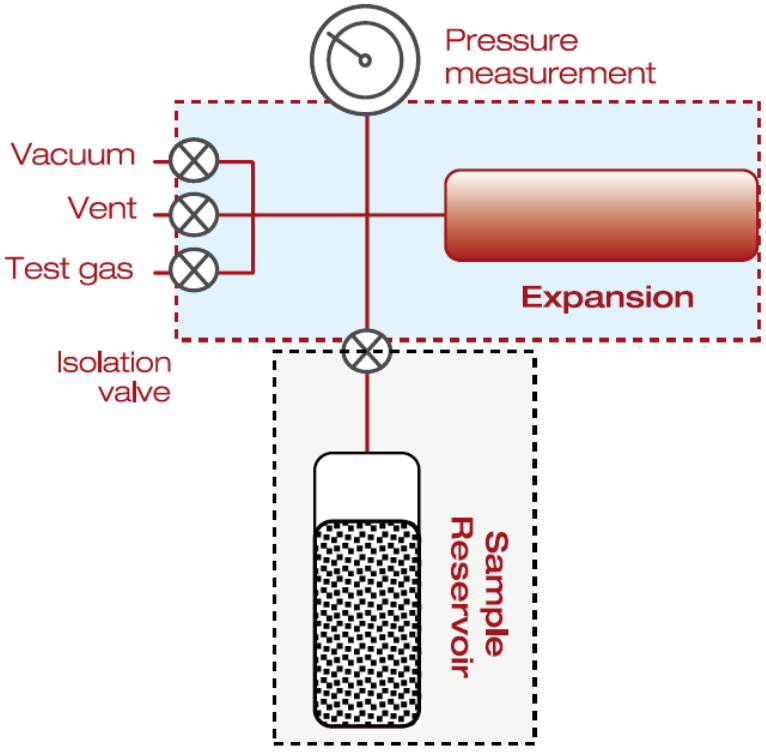

Figure 20. Sorption apparatus PCTPro-2000

4.0 CO_2/H_2 TRANSPORT IN SUPPORTED LIQUID MEMBRANES

Several CO_2-philic polymers were chosen based on their previously determined CO_2 solubility. Although this solubility was measured at extreme pressures in excess of any pressures that would be found in our membrane studies, it provided an idea of the CO_2-philicity of the materials to be tested. The materials tested fit many of the qualifications mentioned earlier for CO_2-philic materials as well as materials which would make highly permeable membranes. The materials which will be studied include linear polyethers, branched polyethers and highly oxygenated/acetylated polymer backbone structures. The permeance of each CO_2-philic polymer listed above was tested as supported liquid membranes as a function of temperature. Testing the polymers as a liquid provides an assessment of the limiting permeability of a membrane composed of the flexible crosslinked polymer, because the crosslinking of the polymer will decrease the diffusivity of the gas through the membrane. Therefore one would expect that the permeability obtained in these supported liquid membrane tests would exceed the permeability of a flexible membrane composed of the crosslinked oligomer.

CO_2 permeability and CO_2/H_2 mixed gas selectivity for supported liquid results are shown in Figures (Figure 21-Figure 29) as a function of temperature.

Overall results at 37˚C are shown in Table 7 in the summary and conclusion section. The temperature at which the membranes were tested was increased until the point at which they no longer displayed significant CO_2 selectivity (selectivity approaching unity), or to the point where

they no longer were thermally stable (evaporative losses of the liquids during the course of the higher temperature experiments). For most membranes this temperature did not exceed 150 ˚C.

4.1 LINEAR AND BRANCHED POLYETHERS

The linear polyethers that were chosen are shown in the materials section and include: PEGDME, PPGDME, PTMEGDAc, PBGDAc, PFPE, PDMS, PAO and GTA. They were tested as supported liquids on the Biodyne support in the constant pressure apparatus at a CO_2/H_2 molar ratio of 1:1. The membranes were tested until they were no longer thermally stable of the selectivity approached unity.

The mixed gas permeability results for PEGDME (MW=500g/mol) showed that at the lowest temperature tested (37 ˚C) the CO_2 permeability was 814 barrers with a selectivity of 11.06. At the highest temperature (150˚C) the CO_2 permeability was 1220 barrers with a selectivity of 1.53. Figure 21 shows the permeability as a function of temperature from 37˚C to 150˚C. Error bars here, and in all plots, represent a standard deviation of multiple measurements.

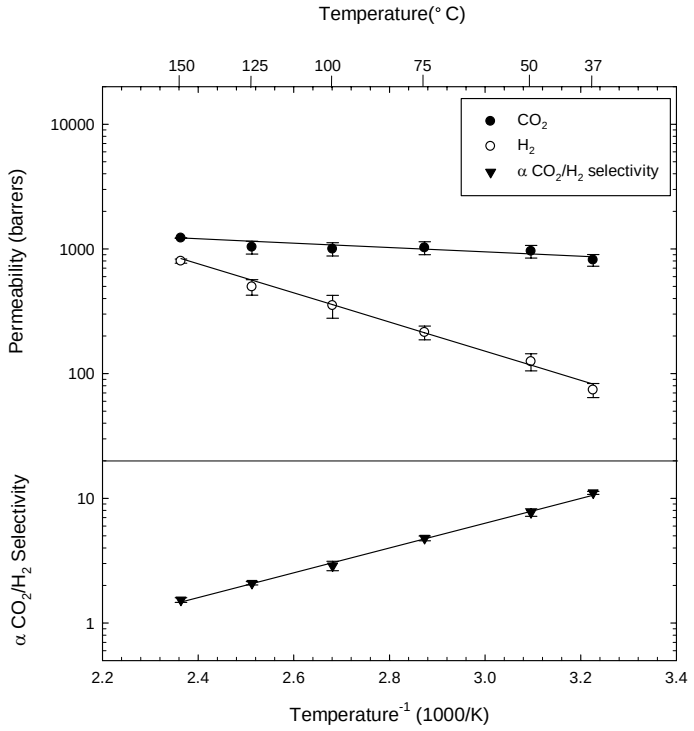

Figure 21. CO_2(●) and H_2(▼) mixed gas permeability as a function of temperature for PEGDME (MW=500 g/mol) supported liquid membrane. The line indicates the exponential fit to determine the permeation activation energy.

The results for PPGDME showed lower permeabilities compared to PEGDME where the CO_2 permeability at the lowest temperature tested (37˚C) was 518 barrers with a selectivity of 5.86 and at the highest temperature (150˚C) the CO_2 permeability was 994 barrers with a selectivity of 1.29. The lower selectivities were probably due to an increase in FFV in a branched version of PPGDME; the decrease in the permeability was more than likely due to the fact that the molecular weight (MW) was slightly higher, which was shown with PFPE and PDMS to cause lower permeabilities as the MW. Matteucci et al. mentioned that the "molecular mass of polymers typically does not significantly influence the gas permeation parameters"; however

with PFPE and PDMS we have shown that the molecular mass can cause a change in the permeability but not a significant effect on the selectivity [1].

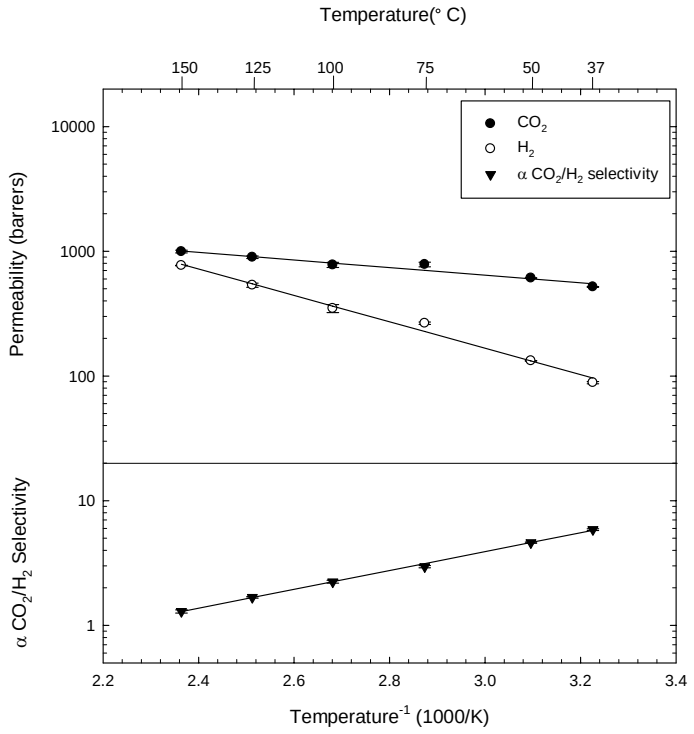

Figure 22. CO_2(●) and H_2(▼) mixed gas permeability as a function of temperature for PPGDME (MW=1060 g/mol) supported liquid membrane. The line indicates the exponential fit to determine the permeation activation energy.

The polybutylene glycol acetate with the linear repeat unit, PTMEGDAc, had a CO_2 permeability of 956 barrers at 37 ˚C and H_2 permeability was determined to be 109 barrers at 37 ˚C, leading to very high mixed gas selectivity value of 8.9; whereas the PBGDAc with the branched repeat unit had a CO_2 permeability of 289 barrers and a selectivity of 3.3. Both of the SLMs with linear monomeric repeat units, PEGDME and PBGDAc, had very high selectivity

values or 11.06 and 8.9, respectively, whereas the significantly lower values of selectivity of 5.9 and 3.3 were associated with the PPGDME and PBGDAc, respectively, both of which possess branched monomeric units.

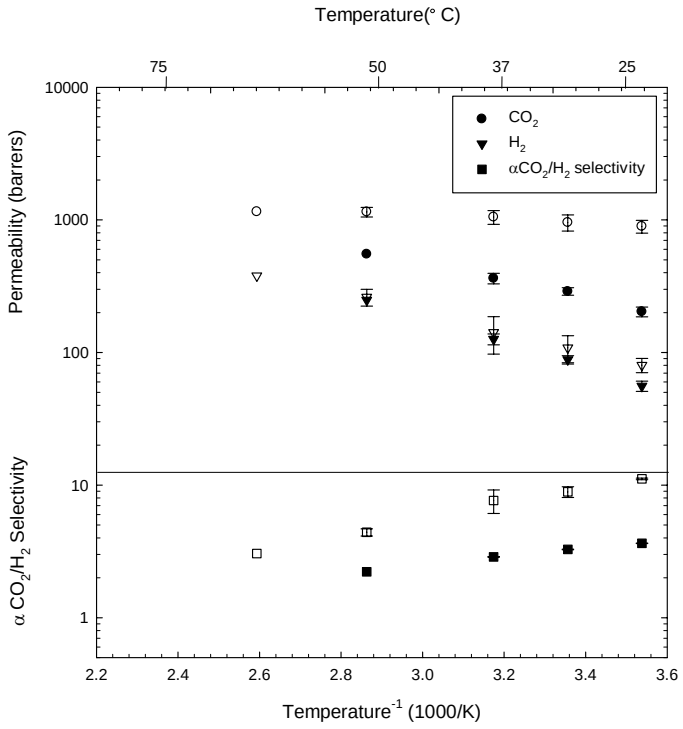

Figure 23. CO_2(●) and H_2(▼) mixed gas permeability as a function of temperature for PTMEGDAc (MW=230 g/mol, open symbols) and PBGDAc (MW=3000 g/mol, branched repeat unit, closed symbols) supported liquid membrane.

PFPE (MW=960 g/mol) was tested as a liquid supported on a cross-linked nylon membrane and tested in a constant pressure apparatus for mixed gas permeability (CO_2/H_2), however due to the low molecular weight and in turn low boiling point of the polymer, the membrane failed at temperatures greater than 37˚C. In order to circumvent this issue a polymer

with a higher molecular weight will be used for further testing. The results for PFPE showed relatively high permeability of 1220 for CO_2 and 418 for H_2; however the selectivity was the lowest obtained thus far with a value of 2.93. Two molecular weights of PFPE were also tested. The first one had a limited operating temperature range; however, it had a relatively high CO_2 permeability of 1220 barrers with the lowest selectivity obtained for any of the SLMs in this study, 2.93 at 37 ˚C. Once a higher operating temperature range PFPE was used the CO_2 permeability dropped to 283 barrers with a CO_2/H_2 selectivity of 2.00, as shown in Figure

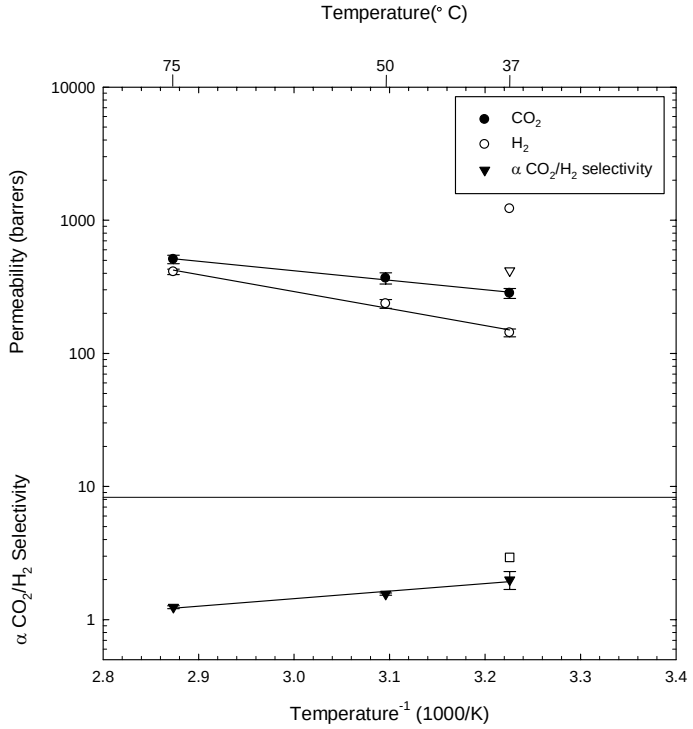

Figure 24. CO_2(●) and H_2(▼) mixed gas permeability as a function of temperature for PFPE (7475 g/mol) supported liquid membrane. The open symbols represent the lower molecular weight PFPE tested (960 g/mol). The line indicates the exponential fit to determine the permeation activation energy.

4.2 OXYGENATED POLYMERS

PDMS (MW=5970 g/mol, MW=770 g/mol) was tested as a liquid supported on a cross-linked nylon membrane in a constant pressure apparatus for mixed gas permeability (CO_2/H_2). The results for PDMS showed similar permeabilities compared to the previously tested PTMEGDAc; however the selectivities were 3-4 times lower. The PDMS CO_2 permeability at the lowest temperature tested (37 ˚C) was 1357 barrers with a selectivity of 3.56 and at the highest temperature (125˚C) the CO_2 permeability was 1324 barrers with a selectivity of 1.14. The lower molecular weight PDMS displayed higher permeabilities; however, the selectivity did not change. The membrane failed at increased temperatures and a higher molecular weight PDMS was chosen to avoid evaporation. Figure 25 shows the average value of permeability and selectivity versus temperature for PDMS with MW=5970 g/mol and MW=770 g/mol. The higher molecular weight PDMS (MW ~6000, 100 cSt) had a CO_2 permeability at 37 ˚C of 1517 barrers with a selectivity of 3.7. The lower molecular weight PDMS (MW ~1000) displayed higher permeability values of 2194 barrers at 37 ˚C; however, the selectivity did not change.

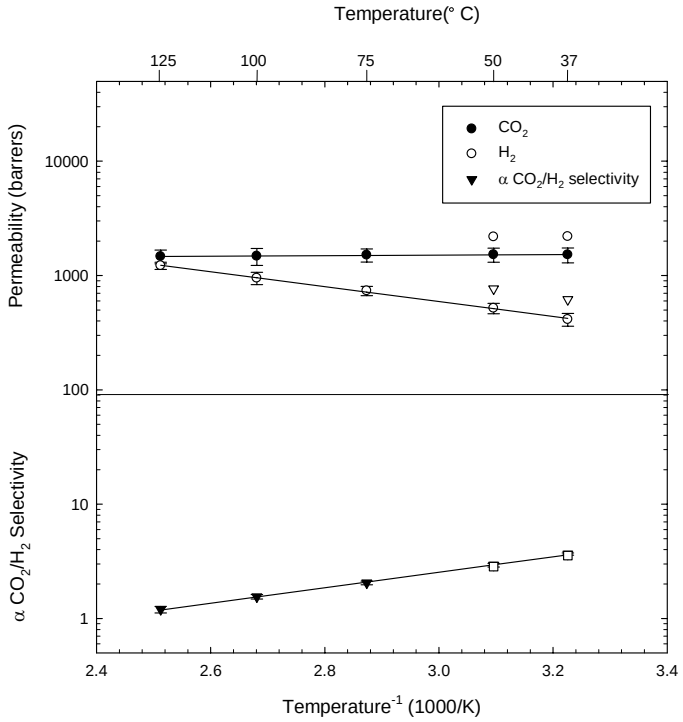

Figure 25. CO_2(●) and H_2(▼) mixed gas permeability as a function of temperature for PDMS (MW=6000 g/mol) supported liquid membrane. The open symbols represent the lower molecular weight PDMS tested (770 g/mol). The line indicates the exponential fit to determine the permeation activation energy.

PAO had the lowest CO_2 permeability of 47 barrers with the second lowest selectivity 3.00 at 37 ˚C, Figure 26. The low permeability and selectivity could be attributed to the high degree of branching within the polymer chain.

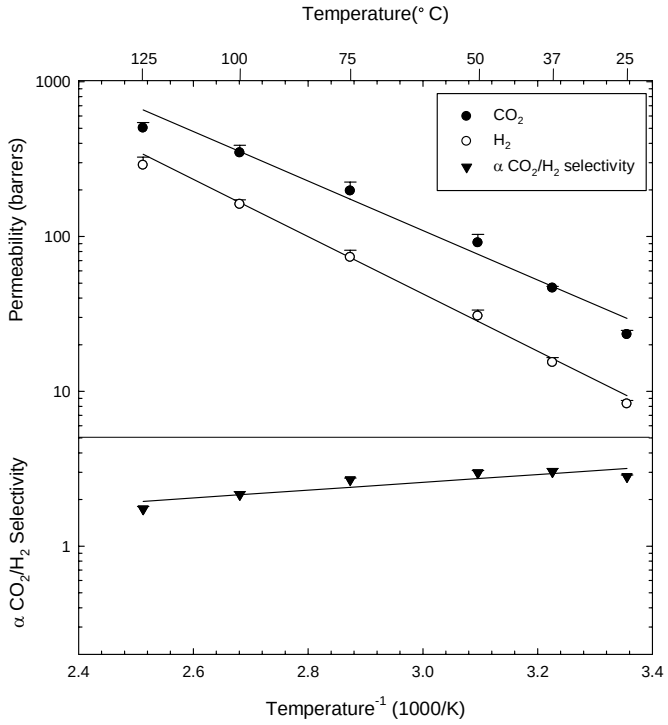

Figure 26. CO_2(●) and H_2(▼) mixed gas permeability as a function of temperature for PAO (MW=345 g/mol) supported liquid membrane. The line indicates the exponential fit to determine the permeation activation energy.

GTA results had very similar results to the PBGDAc, with a CO_2 permeability of 1844 barrers with the third highest selectivity of 8.7 at 37 ˚C. The results for GTA are shown in Figure 27. The solubility of the GTA are shown in the sorption isotherm in Figure 28.

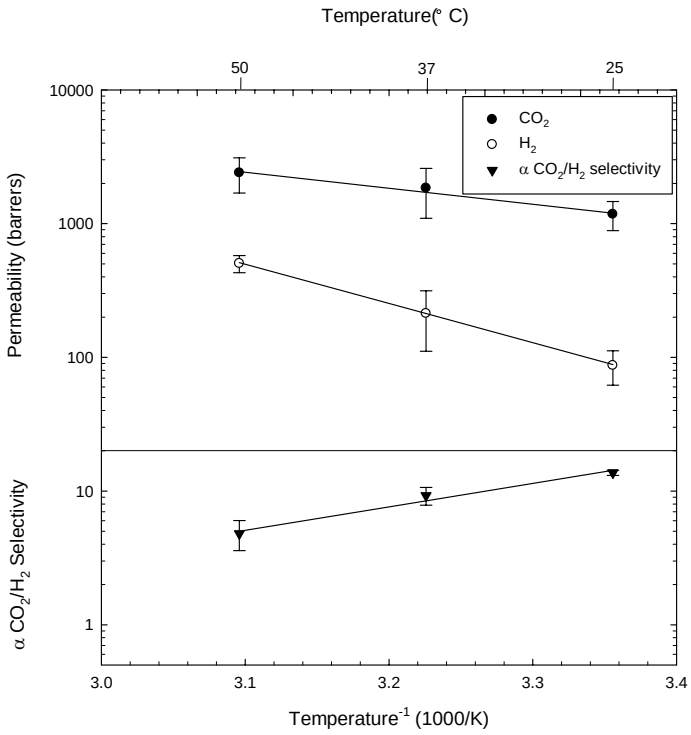

Figure 27. CO_2(●) and H_2(▼) mixed gas permeability as a function of temperature for GTA supported liquid membrane. The line indicates the exponential fit to determine the permeation activation energy.

4.3 SORPTION ISOTHERMS

Sorption isotherms give an idea of the CO_2-philicity at a given pressure and temperature. The sorption results below in Figure 28 are at pressures similar to those used in our mixed gas permeability experiments. The solubility of CO_2 into the polymers is indicated by a larger CO_2 mole fraction sorbed at a given equilibrium pressure. The sorption capacity was measured for PEGDME and GTA at 35˚C and the literature values of solubility for an ionic liquid (IL) [55]. The IL had the highest solubility followed by PEGDME and GTA. The solubility values may

explain the selectivity difference between PEGDME and GTA, since PEGDME achieved a higher selectivity which could be due to a higher solubility selectivity.

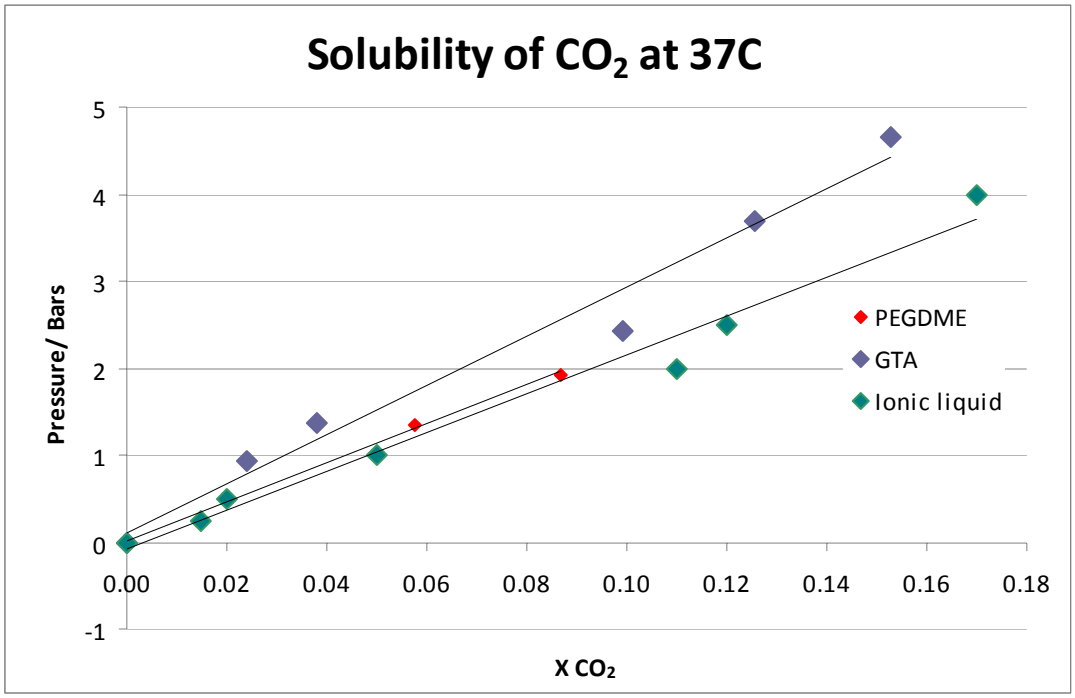

Figure 28. Sorption isotherm for PEGDME, GTA and Ionic Liquid

4.4 TEMPERATURE DEPENDENT TRANSPORT

The permeability temperature dependence can give us an indication of the best temperature the material can be used at to get the highest permeability/selectivity combination. The curves are fitted to determine the activation energy for permeation. The activation energy indicates how

dependent the permeability coefficient is on temperature. The activation energy is calculated from Equation 14, by fitting the permeability curves. The activation energy is calculated from the slope of the plot of ln P vs 1/T, which comes from the linearized version of Equation 14.

$$\ln(P) = \ln(P_o) - \frac{E_p}{RT} \qquad 19$$

For PEGDME the hydrogen permeability and selectivity show strong Arrhenius dependencies; however, the CO_2 permeability has a weak Arrhenius dependence, which could be due to the extremely strong interactions between CO_2 and the polymer. PPGDME, the CO_2 and H_2 permeability and permselectivity show very good Arrhenius dependencies. PTEMGDAc shows a weak Arrhenius dependence for CO_2 permeability, again this maybe due to strong interactions between CO_2 and the polymer. PTMEGDAc has a very good Arrhenius dependence for H_2 permeability. The PBGDA has a very good Arrehnius dependence for both CO_2 and H_2. PFPE show Arrehnius dependence for both CO_2 and H_2 permeability; however, the activation energies are similar indicating that CO_2 and H_2 are not selective to either gas. The Arrhenius plot for PDMS shows that the H_2 permeability and selectivity follow an Arrhenius dependency; however the CO_2 permeability does not show Arrhenius dependence and has the lowest slope for all of the polymers. The CO_2 permeability barely changes as a function of temperature. As temperature increases, the permeability is expected to increase due to a higher diffusion coefficient; however, with PDMS which has a strong intermolecular interaction with CO_2 (therefore increased solubility), the balance between solubility decreases with increasing temperature and diffusivity increases must be balanced as the temperature increases. PAO and GTA have high activation energies leading to strong temperature dependence for permeation.

The H_2 mixed gas permeability results for the SLMs over the 27-150˚C temperature range exhibit a strong Arrhenius relationship, increasing dramatically with temperature. The

increase in H_2 permeability with temperature in these membranes where both CO_2 and H_2 are permeating may be attributed to an increase in the diffusivity of H_2 with temperature and/or the increasing solubility of hydrogen in the polymer [56-58]. The CO_2 permeability values, however, especially those for PDMS, display a very slight increase over the same temperature range. Apparently, as temperature increases, the increase in diffusivity of CO_2 is mitigated by the decrease in the solubility of the CO_2 [40]. Solubility and diffusivity values were not determined during this study, however. Regardless of the causes, in all cases the mixed gas selectivity decreases significantly with increasing temperature, which indicates that the most effective gas separations occur at the lowest temperature.

Table 6. Activation energies

Polymer	$Ea_p(CO_2)$ (kJ/mol)	$Ea_p(H_2)$ (kJ/mol)
PEGDME	3.36	22.4
PPGDME	5.84	20.3
PTMEGDAc	3.30	19.5
PBGDAc	16.9	25.4
PFPE	13.7	22.4
PDMS	0.44	12.8
PAO	30.6	35.5
GTA	22.9	56.2

4.5 H_2S CONTAMINANT

Although most of the testing proposed will be conducted on gas mixtures consisting of only the two primary gas constituents relevant to the proposed separation technology (e.g. CO_2/H_2 for pre-combustion separation), contaminants are ubiquitous in most industrial separations. These contaminants can decrease the permeability and selectivity of these polymeric membranes if they react with the contaminant. It is also possible that the contaminant can permeate the membrane or be retained primarily in the retentate. Although the levels of contaminants considered in this study will be too low to determine the permeability of the membrane to the impurity, its effect (if any) on the ability of the membrane to separate the main gas constituents will be determined. H_2S will be the foremost model impurity because of its presence in the effluent of coal gasifiers.

The mixed gas permeability and selectivity of PEGDME with and without H_2S is shown in Figure 29. The effect of H_2S was shown for PEGDME and indicated that there was no difference for this particular polymer which was expected due to the fact that the PEGDME is typically the main constituent in Selexol and Selexol is used to remove acidic gases from contaminated streams.

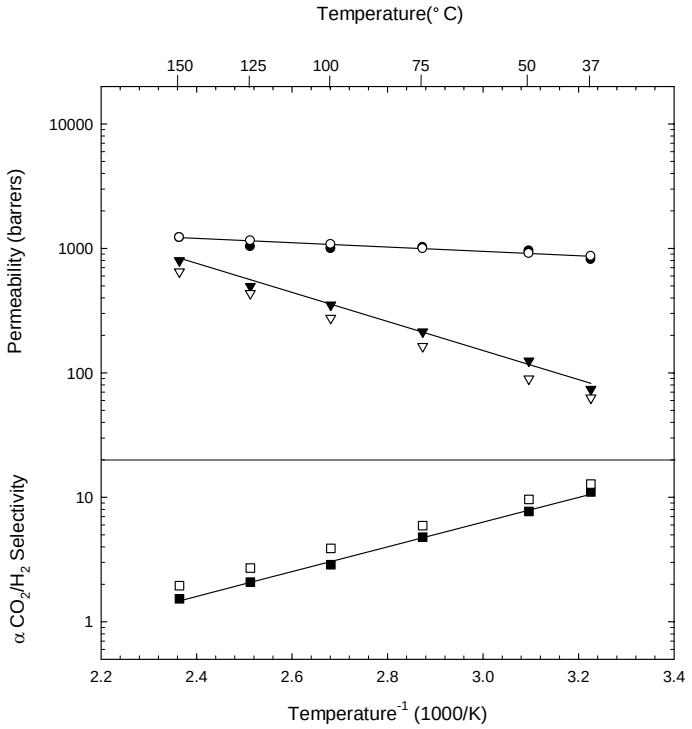

Figure 29. CO_2(●) and H_2(▼) mixed gas permeability as a function of temperature for PEGDME (MW=500 g/mol) supported liquid membrane in a stream containing 500 ppm H_2S. The figure shows that there is no significant difference between the permeability and selectivity when H_2S is added to the gas stream.

4.6 SUMMARY AND CONCLUSIONS

The overall results for permeability and selectivity are shown in Table 7. The most promising SLMs appear to be PEGDME, PBGDAc and GTA which had permeability values on the order of 1000 barrers with selectivities of roughly 10 at 37 ˚C.

Generally the permeability will increase as temperature increases due to the increase in the diffusion coefficient as a function of temperature; however, temperature will cause a decrease

in the solubility selectivity simply because the solubility of gases decreases with increasing temperature. Based on the permeation activation energies listed in Table 6, PDMS shows the lowest temperature dependency for CO_2 permeation and PAO permeation has the highest dependence on temperature, whereas for H_2 permeation GTA has the highest temperature dependence and PDMS again has the lowest temperature dependence.

Table 7. Overall SLM Mixed Gas Results at 37° C

Polymer	Type	CO_2 permeability (barrers)	H_2 Permeability (barrers)	CO_2/H_2 Mixed Gas Selectivity
PEGDME	SLM	814	74	11.1
PTMEGDAc	SLM	956	109	8.9
GTA	SLM	1844	213	8.7
PPGDME	SLM	518	88	5.9
PDMS(5 cSt)	SLM	2194	617	3.6
PDMS(100 cSt)	SLM	1517	414	3.7
PBGDAc	SLM	289	88	3.3
PFPE GPL100	SLM	1220	418	2.9
PFPE GPL107	SLM	283	143	2.0
PAO	SLM	47	16	2.9

5.0 CO_2/H_2 TRANSPORT IN SOLID/CROSSLINKED MEMBRANES

5.1 SOLID MEMBRANES

PFA, PVAc, and PFA are considered to be extremely CO_2-philic because they melt and then dissolve in liquid and supercritical CO_2 as pressure is increased to very high pressures (e.g. 2000 – 25000 psia). PVAc and PLA have previously been tested and have exhibited very low permeability values due to their glassy nature (Table 8), with both materials exhibiting H_2-selectivity rather than CO_2-selectivity. The PFA membrane associated with this study had a mixed gas permeability of 62 barrers for CO_2 and 45 barrers for H_2 at 25˚C leading to a CO_2/H_2 selectivity value of 1.38 [59]. Despite the CO_2-philicity of these polymers as evidenced by their dissolution in dense CO_2, the polymers exhibit disappointingly low CO_2 permeability. This may be attributed to low CO_2 diffusivity of these gases through the polymer, and/or a low solubility of the CO_2 in the solid polymers because they are not molten at these low levels of CO_2 partial pressure. At elevated pressure these polymers melt prior to dissolving into CO_2. Neither solubility nor diffusivity were measured in this study, however; only permeability and selectivity.

Table 8. Permeability and selectivity results for solid CO_2-philic polymers

Polymer	Temperature (˚C)	CO_2 Permeability (barrers)	H_2 Permeability (barrers)	CO_2/H_2 Selectivity	Ref
PVAc	30.4	1.5	-	-	[60]
PVAc	30	15.1	13.1	0.87	[61]
PLA	30	10.2	-	-	[62]
PLA	35	1.27	6.23	0.20	[63]
PFA	25	62	45	1.38	This work
Teflon AF/Krytox	25	381	196	1.94	This work

PFPE plasticized Teflon AF2400 (70/30 wt%) was tested as a mixed matrix film membrane (film thickness 60 μm) and tested in the constant pressure apparatus for mixed gas permeability (CO_2/H_2/bal Ar). Although Teflon AF2400 is CO_2-insoluble, PFPE is highly CO_2 philic polymer. Table 9 shows the CO_2 and H_2 permeability and CO_2/H_2 selectivity for PFPE plasticized Teflon AF2400 (70/30 wt%), pure PFPE samples at 25˚C at a differential pressure of 1 atm. Literature data is also shown for Teflon AF 2400 at 25˚C and a feed pressure of 50 psig and a permeate pressure at atmospheric [47]. The CO_2 permeability of the membrane dropped to ~400 barrer at 25˚C and is comparable to the supported liquid membrane made of pure PFPE; however the selectivity of the Teflon AF was slightly enhanced from 1.18 to 1.94, but with a corresponding decrease in the CO_2/H_2 selectivity compared to pure PFPE.

Table 9. Results of Plasticized Teflon, Krytox and Teflon

Polymer	CO_2 Permeability (Barrers)	H_2 Permeability (Barrers)	CO_2/H_2 Selectivity
70 wt%PFPE/ Teflon AF2400	381	196	1.94
Krytox GPL 107 MW 7475 g/mol	300	136.0	2.21
Krytox GPL 100 MW 960 g/mol	1220	418	2.93
Teflon AF 2400 [47]	3900	3300	1.18

5.2 CROSSLINKED MEMBRANES

The corresponding crosslinked membranes were also tested for CO_2/H_2 mixed gas permeability as a function of temperature. Figures (9-13) show the permeability and mixed gas selectivity as a function of temperature for crosslinked membranes of PEG, PPG, PBG, PDMS, and PFPE, respectively. Overall results at 37˚C are shown in Table 4.

The PEGDA results, Figure 30, exhibits a CO_2 permeability of 52 at 37 ˚C, with a H_2 permeability of 10.9 barrers, which leads to a mixed gas selectivity of 4.72 at 37 ˚C. The permselectivity was halved from 11.06 for the corresponding PEGDME SLM analog which is more than likely due to the blockage of polymer volume by the crosslinks.

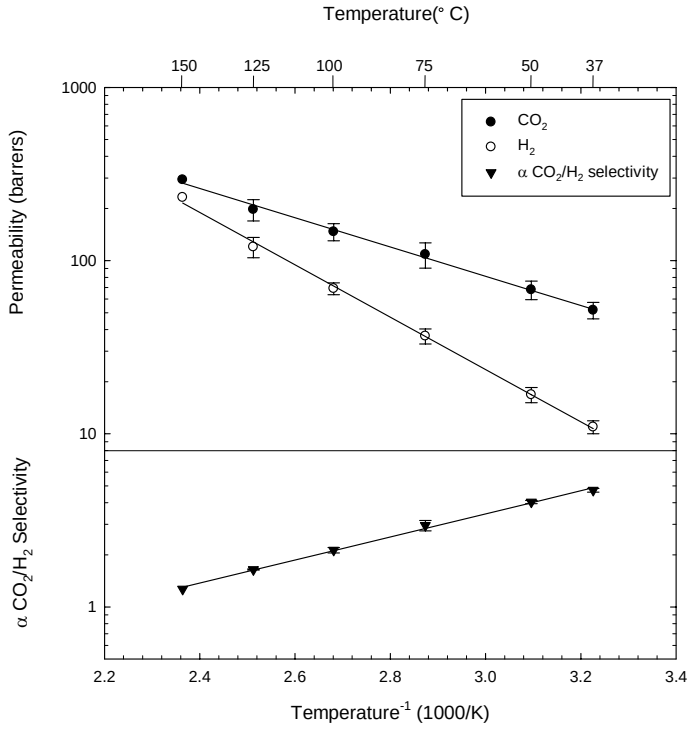

Figure 30. CO_2(●) and H_2(▼) mixed gas permeability as a function of temperature for PEGDA (MW=700 g/mol) crosslinked membrane. The line indicates the exponential fit to determine the permeation activation energy. Literature values for photocured PEGDA are available in reference [64].

The PPGDA crosslinked membrane results, Figure 31, exhibited a CO_2 permeability of 103 at 37 ˚C. The H_2 permeability was 36 barrers at 37 ˚C, which leads to a mixed gas selectivity value of 2.83. The mixed gas selectivity decreased from 5.86 in the PPGDME SLM to 2.83 in the cross-linked PPGDA membrane at 37 ˚C, while the CO_2 permeability decreased five times from 518 barrers to 103 barrers at 37 ˚C.

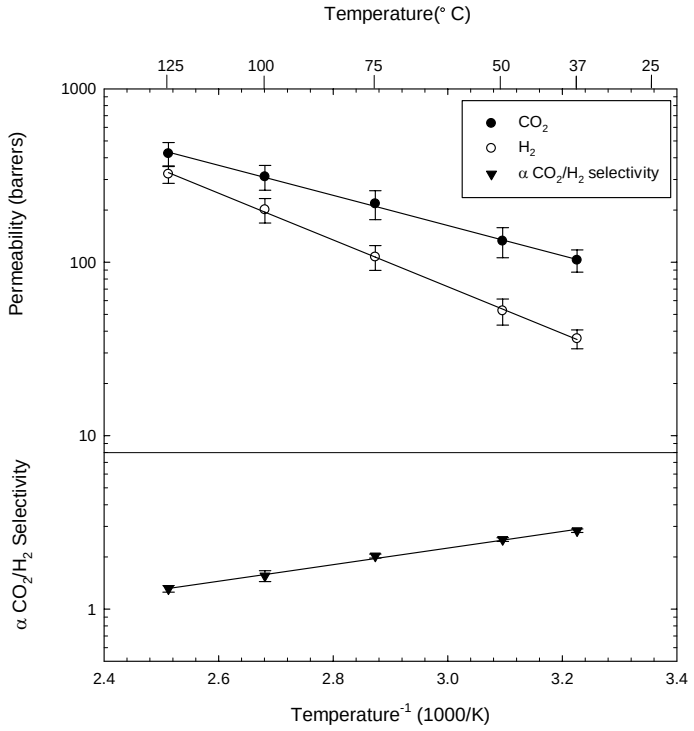

Figure 31. CO_2(●) and H_2(▼) mixed gas permeability as a function of temperature for PPGDA (MW=900 g/mol) crosslinked membrane. The line indicates the exponential fit to determine the permeation activation energy.

Membranes composed of crosslinked polybutylene glycol with branched repeat unit (PBGDA) and a linear monomeric unit (PTMEGDA) were also assessed for CO_2 and H_2 permeability values, Figure 32. The CO_2 permeability for the PTMEGDA was 299 at 25 ˚C and the H_2 permeability was determined to be 44 barrers at 25 ˚C, which leads to and a permselectivity of 6.83; however the results for PBGDA are much lower having a CO_2 permeability of 17 and a selectivity of 2.30. The results for the PTMEGDA are excellent relative to all of the other crosslinked membranes, yielding the highest selectivity and the second-highest permeability (second only to the low selectivity, crosslinked PDMS membrane).

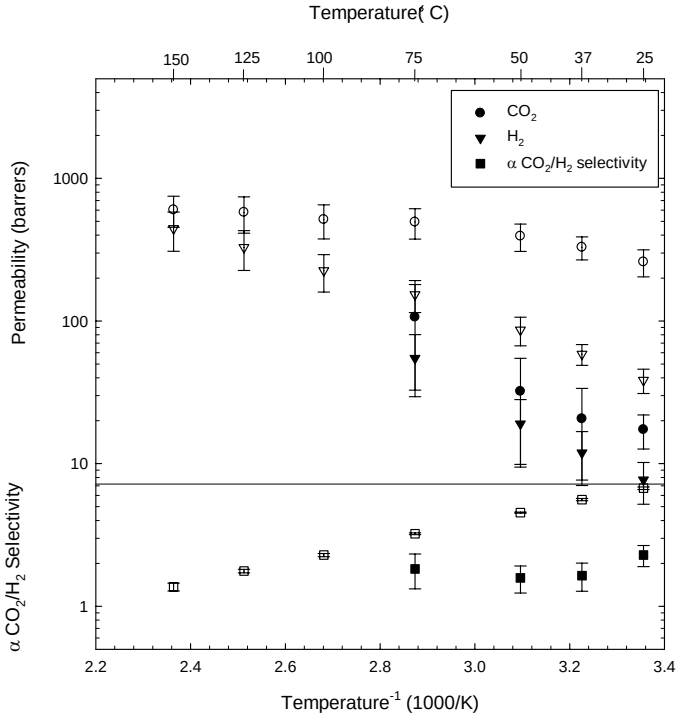

Figure 32. CO_2(●) and H_2(▼) mixed gas permeability as a function of temperature for PTMEGDA(open symbols) and PBGDA(closed symbols) crosslinked membranes.

Crosslinked PDMS had a CO_2 permeability of 2848 barrers and a CO_2/H_2 selectivity of 3.5 at 37 ˚C, Figure 33. Compared to the PDMS SLM values of 2194 barrers and 3.7, the commercial crosslinked PDMS membrane actually had higher permeability and selectivity

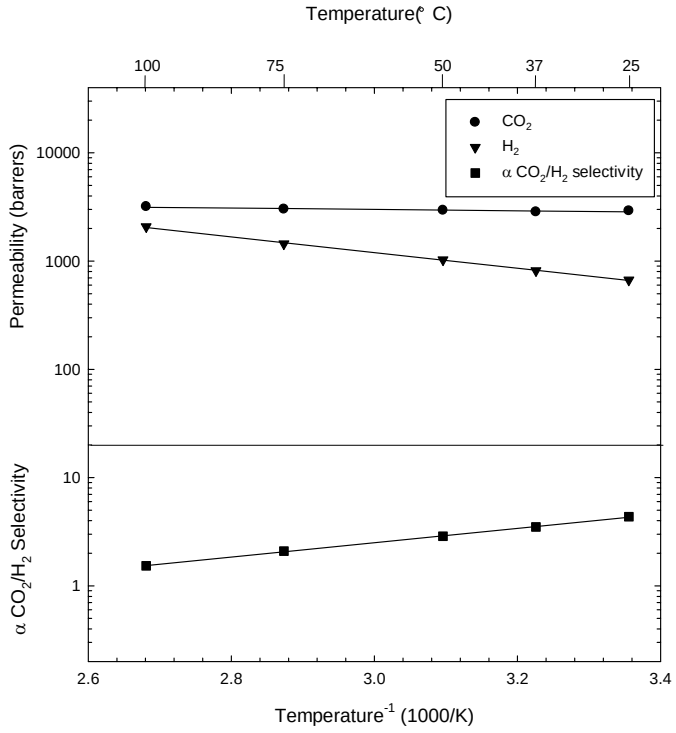

Figure 33 CO_2(●) and H_2(▼) mixed gas permeability as a function of temperature for PDMS crosslinked membrane. The line indicates the exponential fit to determine the permeation activation energy.

For the crosslinked PFPE membranes, the CO_2 permeability was 338 at 37 ˚C, while the H_2 permeability was determined to be 203 barrers at 37 ˚C, which leads to a permselectivity of 1.67 (Figure 34). This value is the lowest CO_2/H_2 mixed gas selectivity obtained for any SLM or crosslinked membrane in this study. Compared to the lower molecular weight PFPE SLM, the crosslinked PFPE membrane showed lower permeability and selectivity at 37 ˚C.

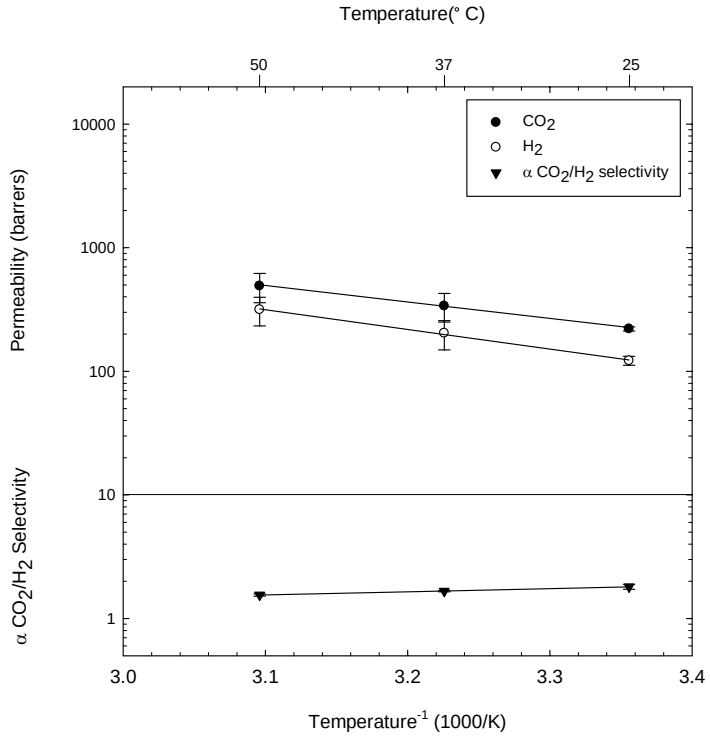

Figure 34 CO_2(●) and H_2(▼) mixed gas permeability as a function of temperature for PFPE crosslinked membrane. The line indicates the exponential fit to determine the permeation activation energy.

5.3 SUMMARY AND CONCLUSIONS

The overall results for crosslinked membranes at 37˚C are shown in Table 10. As was the case in the SLM results, the selectivity values of 4.7 and 5.6 for the crosslinked membranes were greatest for membranes based on PEG and PTMEG, respectively; the two polymers with linear (non-branched) monomer units. The selectivity values of the crosslinked membranes based on branched monomers, PPG and PBG, were half as much at only 2.8 and 1.64, respectively.

Table 10. Overall XLM Mixed Gas Results at 37° C

Polymer	Type	CO_2 permeability (barrers)	H_2 Permeability (barrers)	CO_2/H_2 Mixed Gas Selectivity
PTMEGDA	Xlinked	329	58.6	5.6
PEGDA	Xlinked	52	11	4.7
PDMS	Xlinked	2848	813	3.5
PPGDA	Xlinked	103	36	2.8
PFPE	Xlinked	338	203	1.7
PBGDA	Xlinked	21	12	1.8

6.0 SUMMARY AND CONCLUSIONS

Figure 35 is a plot of CO_2 permeability vs. mixed gas CO_2/H_2 selectivity for polymeric membranes that summarizes our results and literature results for CO_2-selective (reverse selective membrane materials). Our results are shown at 37 ^{0}C and the literature results at comparable temperature values (23-40 ˚C). (The highest selectivity value reported for this separation of ~30 corresponds to PEGDA/PEGMEA membrane at -20 ^{o}C [10], which is well below the temperature range selected for the comparison shown in Figure 12.) An ionic liquid [hmim][Tf_2N] SLM [52] was also included because these membranes also transport CO_2 and H_2 via the solution-diffusion mechanism.

(1) In our study of SLMs, PDMS has exhibited the highest permeability values with modest selectivity, while the PEG-based membranes exhibit the highest selectivity values at lower permeability. The PTMEG-based SLM had similar permeability values relative to the PEG-based SLM, but with a slightly lower selectivity. The greatest selectivity values of 5 – 10 are attained with PEG SLM, PPG SLM, PTMEG SLM, crosslinked PEG, crosslinked PTMEG, ionic liquids, [hmim][Tf2N] supported ionic liquid, PEBAX, PEBAX/PEG, and polyphosphazene. The permeability of these membranes range from ~100 to ~1000 barrers.

Further, the crosslinked PTMEG membrane was superior to the other candidates, exhibiting the highest selectivity and the second-highest permeability. Crosslinked PEG had a slightly lower

selectivity and a lower permeability. When the SLM and crosslinked versions of the same PEG, PPG and PBG polymers are compared, it is apparent that crosslinking substantially reduces the permeability and selectivity, but yields a more resilient flexible membrane that will not slowly evaporate as the liquid in a SLM would.

When the results of this study and literature results are assessed on the plot of CO_2/H_2 selectivity vs CO_2 permeability in the 23-40 ^oC temperature range, it is apparent that:

(2) Selectivity values drop from ~10 to ~1 as the CO_2 permeability increases from ~100 - ~10000 barrers. For example, PDMS-based polymers have selectivity values of 3 - 4 and permeability values of ~1000 - ~3000, while polymers of ultra-high free volume such as poly(4-methyl 2-pentyne) has a permeability of ~20000 barrers and a selectivity of only ~2.

(3) The polymers that have the highest permeability of ~100 barrers while maintaining the highest selectivity of roughly 10 include PEG-based membranes, PTMEG-based membranes, polyphosphazene, and [hmim][Tf2N] supported ionic liquid membranes.

(4) Highly CO_2-philic polymers do not necessarily yield highly permeable, CO_2-selective membranes for the CO_2/H_2 separation. Very good membranes can be obtained with crosslinked or supported liquid PEG or PTMEG. The PPG-based and PBG-based membranes did not perform as well as either the PEG-based or the PTMEG-based membranes, possibly because of the branching in the PPG and PBG monomer. PDMS yields a very high permeability, but low selectivity membrane. PFPE-based membranes suffered from very low selectivity. PAO membranes exhibited very low selectivity and low permeability. Extremely low permeability cast membranes result

when they are composed of high molecular weight, low melting point polymers (PFA, PVAc, and amorphous PLA).

Despite being extraordinarily CO_2-philic, the solid polymers, PFA, PVAc, PLA, did not yield highly CO_2-selective or permeable cast membranes, possibly due to the low diffusivity of the CO_2 in these polymers.

The greatest values of CO_2 permeability and CO_2/H_2 selectivity were exhibited by the SLMs. In particular, PEGDME, PTMEGDAc, and PDMS membranes exhibited better performance than PPGDME, PBGDAc, PFPE, or PAO-based SLMs. Of the three most promising polymers, at 37 ˚C the PEGDME SLM had the greatest mixed gas selectivity (~11) and lowest CO_2 permeability (~900 barrers), PDMS had the highest permeability (~2000 barrers) but lowest permselectivity (~3.5), and PTMEGDAc had intermediate values of both CO_2 permeability (~955 barrers) and mixed gas selectivity (~9). Crosslinked versions of the PEG, PTMEG and PDMS polymers at 37 ^oC exhibited selectivity values of ~ 5, 6 and 3.5, respectively, and CO_2 permeability values of ~50, 300, and 3000 barrers, respectively.

In both the SLM and crosslinked membranes, the polymers with linear monomeric repeat units, PEG and PTMEG, yielded markedly better results than the membranes composed of polyethers with branched monomeric units, PPG and PBG.

Future tests will contrast the results of PPG, which has a branched repeat unit, with polytrimethylene ether glycol, which is based on $–((CH_2)_3O)-$, in order to confirm whether the linear architecture of the monomeric unit yields better membrane performance.

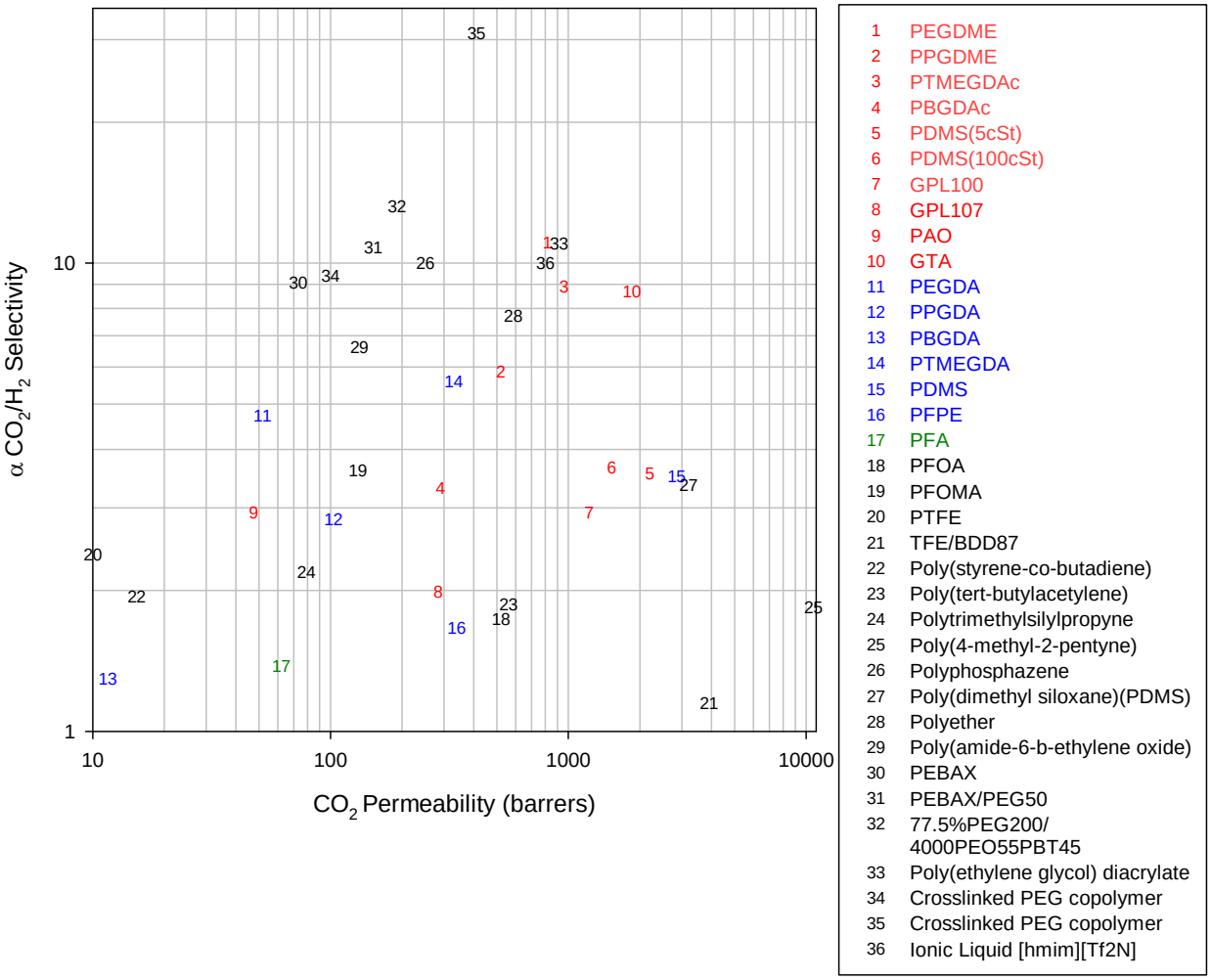

Figure 35. Literature data for mixed gas CO_2/H_2 separation factor versus CO_2 permeability for CO_2 selective membrane. Data from this study corresponds to results at 37 ^oC (red-SLM, blue-crosslinked, green – solid), while the literature results (black) for CO_2/H_2 separation factor versus CO_2 permeability at temperatures of 23 – 40 ^oC (PFOA and PFOMA[59], PTFE[65], TFE/BDD87[66], poly(styrene-co-butadiene) [65], PTBA[35], PTMSP[67], PMP [35], Polyphosphazene[27], PDMS[68], Polyurea-Polyether [36], PEBAX[37], PEBAX/PEG50[37], PEG200/PEO-PBT[69], PEGDA[70], Crosslinked PEG copolymer[10], Ionic Liquid [51])

7.0 FUTURE WORK

The future work for CO_2 selective membranes requires that membrane materials become more selective or that the selectivity requirements get lowered. Some of the ways that higher permeability as well as mixed gas selectivity can be obtained is by using more realistic pressures and compositions, using new materials, and using new membrane configurations.

7.1 PRESSURE/HUMIDITY DEPENDENCE ON PERMEATION

In the real process of pre-combustion CO_2 capture from the IGCC process contains humidity as well as being at a significantly higher pressure from the conditions used in this study. It has been shown that an increase in pressure can enhance the permeability [71]. This is generally due to the increase in the solubility parameter according to Henry's law. Unlike glassy polymers rubber polymers generally show an increase in permeability as a function of increased pressure [1]. Humidity can also cause free volume increase in particular glassy polymers; however, with a rubbery material such as PDMS the competitive sorption of H_2O occurs lowering the permeability of individual gas components CO_2 and N_2[72, 73]. It would be desirable to keep the water on the retentate side with the hydrogen because of the increased volume that would be expanded over the turbine. It would also have to be determined if the increased permeability would be accompanied by a loss of selectivity.

7.2 PRESSURE SWING ABSORPTION

Membrane contactors can be used to selectively absorb gases using a physical solvent. Essentially they operate by using a non-wetting porous membrane which is in contact with the gas and the liquid can be used to selectively remove gases due to a partial pressure difference between the dissolved gas and the pressure in the gas stream. Typically these membranes are being used to remove dissolved gases from water [ref]. Since our materials are essentially the solvents used in pressure swing absorption(PSA), the membrane configuration would allow the use of these materials and have a larger surface to volume ratio versus a packed bed column and should have the ability to purify the gas stream as much as a PSA. The configuration would need a membrane "absorber" and also a regeneration membrane setup. For these membranes there are some design considerations that must be accounted for such as the non-wettability of the hollow fiber materials, the breakthrough pressure (surface tension and contact angle can be used to determine this), the shell-tube configuration and flowrates. The method of operation would still be Henry's Law for sorption. Scale up should also be easy due to the modular nature of the membrane units.

7.3 NEW MATERIALS

Since we tested polymers that had both linear and branched backbones from C2-C4 we would have liked to include a new product which is currently a proprietary compound produced by Dupont under the trade name Cerenol. Cerenol is essentially a linear C3 polyether (the monomer is linear, -($CH_2CH_2CH_2O$)-) that is produced sustainably from corn, according to DuPont. This

polymer would help us to assess whether this "linear" polyether would, upon crosslinking, exhibit outstanding permeability and selectivity just like the crosslinked "linear" PEG- and PTMEG-based polyethers. Despite 11 months of negotiations for a materials transfer agreement between Pitt and DuPont lawyers, these Cerenol samples have still not been obtained. Our attempts to synthesize this polymer from 1,3-propane diol were unsuccessful.

Another material which could be of interest for this separation is a linear PPG or PTMEG + polyamide [NH-$(CH_2)_5$-CO], similar to PEBAX™®, which is a copolymer of PEG and polyamide. The polymer here would contain the linear PPG homopolymer as the rubbery material and the amide would be used as the glassy material. The rubbery matrix would enhance the permselectivity where as the glassy matrix would allow the material to maintain improved chemical and mechanical integrity. Since the permeability of the PTMEGDA was higher than PEG, it is possible that the PPG should also produce a membrane with higher permeability and selectivity. It was also shown that the incorporation of Selexol > 20 wt% allowed the PEBAX material to become more permeable and more selective due to the increase in free volume [74].

7.4 TEST CO_2/N_2 PERMEABILITY

Since the materials chosen for this separation were shown to work moderately well for CO_2/H_2 separation, they would work remarkably better for the CO_2/N_2 separation. The separation for CO_2/N_2 is interesting for post-combustion separation for the IGCC process. The permeability selectivity increases dramatically for CO_2/N_2 because there is less of a size selective nature for this separation. For example the selectivity for PDMS shows a 3x increase in selectivity while maintaining high permeability[75].

APPENDIX A

COMPRESSIBLITY

The following pressure and temperature dependent compressibility factor equations were used to make sure that the use of pressure instead of fugacity was appropriate. A plot of the compressibility was calculated using the pressure and volume data at isothermal conditions show on National Institute of Standards and Technology (NIST) chemistry webbook.

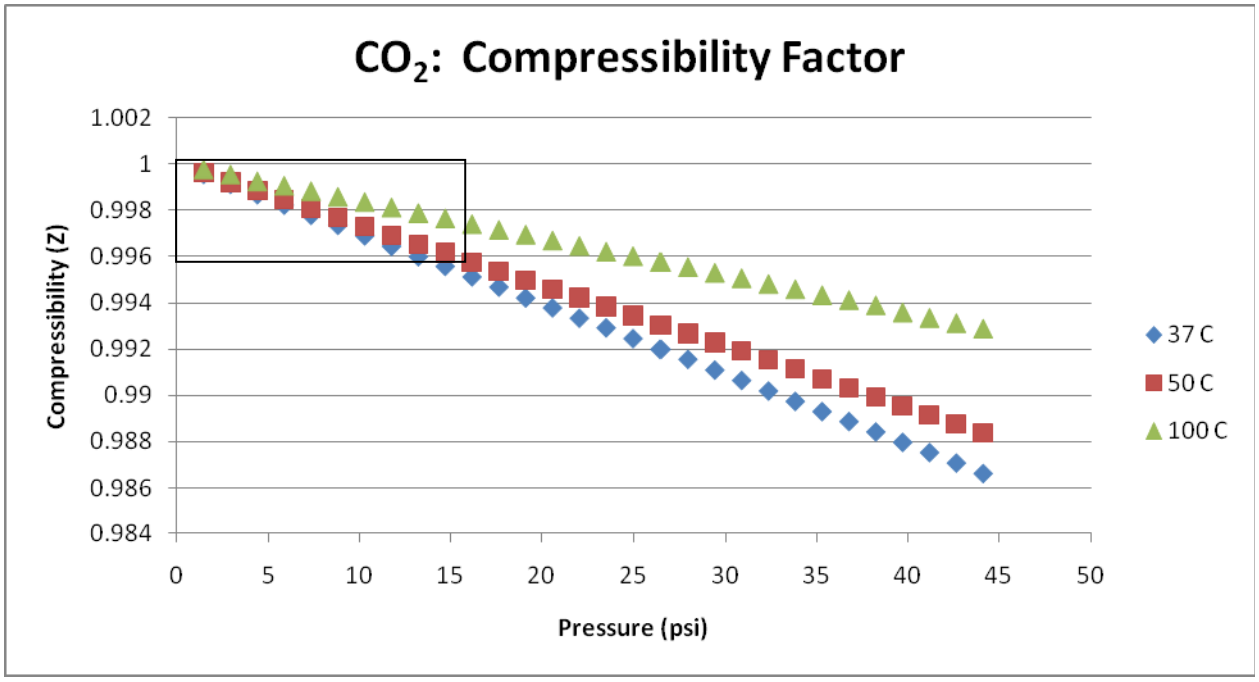

The rectangle shows the compressiblity factor in our experiments and indicates that it is still quite low and our assumption of ideal gas still applies.

The compressibility factor can be calculated based on the equations below where p is the pressure in psia.

37°C: $Z = 1.5842E\text{-}09p^3 - 1.6049E\text{-}07p^2 - 2.9873E\text{-}04p + 1.00$

50°C: $Z = -2.2968E\text{-}09p^3 + 8.9865E\text{-}08p^2 - 2.6339E\text{-}04p + 1.00$

100°C: $Z = -5.6675E\text{-}09p^3 + 3.1945E\text{-}07p^2 - 1.6494E\text{-}04p + 1.00$

APPENDIX B

NMR DATA: PREPARATION OF POLY(GLYCIDOL)

^{1}H Proton NMR

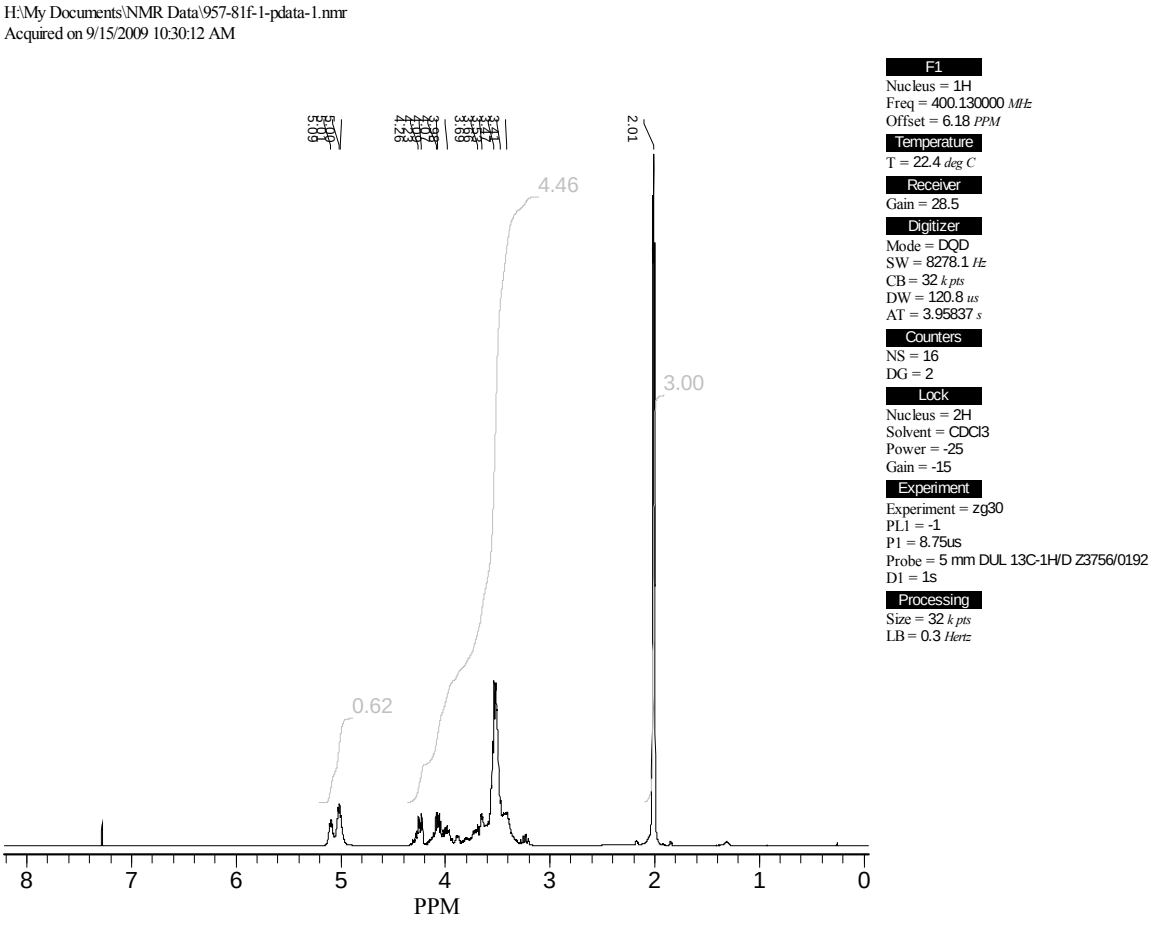

Blow up of hydroxyl region

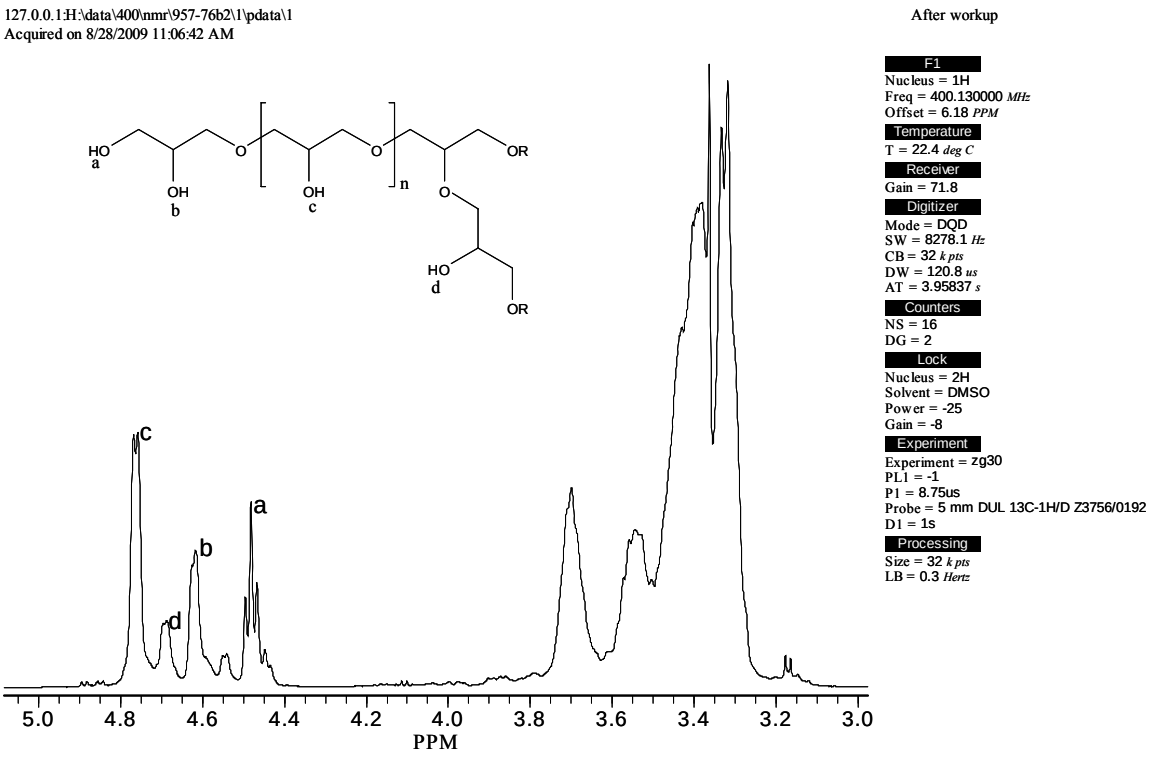

^{13}C Carbon NMR

H:\My Documents\NMR Data\957-81fc-1-pdata-1.nmr
Acquired on 9/15/2009 10:32:39 AM

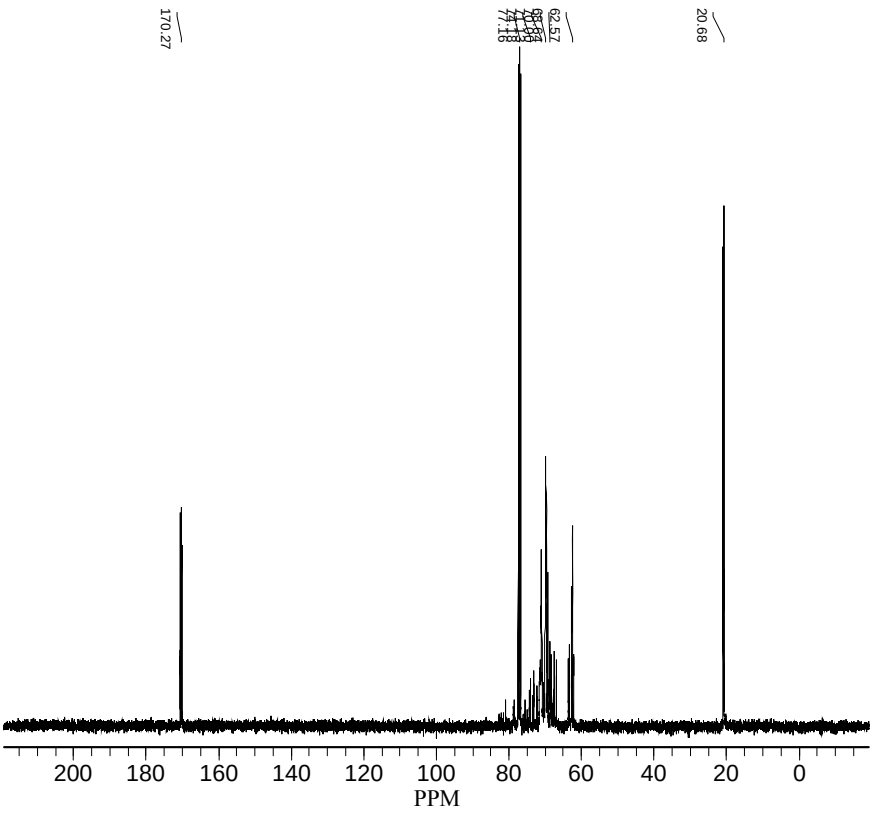

F1
Nucleus = 13C
Freq = 100.612769 *MHz*
Offset = 100.00 *PPM*

F2
Nucleus = 1H
Freq = 400.131601 *MHz*
Offset = 4.00 *PPM*
Modulation = 0 - 180

Temperature
T = 22.4 *deg C*

Receiver
Gain = 32768

Digitizer
Mode = QSIM
SW = 24.0 *kHz*
CB = 16 *k pts*
DW = 41.7 *us*
AT = 683.213 *ms*

Counters
NS = 800
DG = 0

Lock
Nucleus = 2H
Solvent = CDCl3
Power = -25
Gain = -15

Experiment
Experiment = zgpg30
PL1 = -1
PL2 = -1
P1 = 11us
Probe = 5 mm DUL 13C-1H/D Z3756/0192
PL12 = 20.16
D1 = 316.7372us
PL13 = 20.16

Processing
Size = 32 *k pts*
LB = 1 *Hertz*

BIBLIOGRAPHY

1. Yampolskii, Y.P., I.; Freeman,B. D. , ed. *Materials Science of Membranes for Gas and Vapor Separation*. 2006, John Wiley & Sons, Ltd: West Sussex, England.

2. van Amerongen, G.J., *Diffusion in Elastomers.* Rubber Chemistry and Technology, 1964. **37**: p. 1065-1153.

3. Herzog, H., *An Introduction to CO_2 Separation and Capture Technologies*. 1999, MIT Energy Laboratory.

4. Romanosky, R., *Fossil Energy Advanced Materials Program*. 2008, National Energy Technology Laboratory: Pittsburgh.

5. Marano, J.J. and J.P. Ciferino, *Integration of Gas Separation Membranes with IGCC Identifying the right membrane for the right job.* Energy Procedia, 2009. **1**(1): p. 361-368.

6. *Energy Northwest Technical Overview: Pacific Mountain Energy Center and Integrated Gasification Combined Cycle* [cited; Available from: http://www.energy-northwest.com/generation/igcc/technical.php.

7. Ciferno, J.P. and J.J. Marano, *Gas Separation Membrane R&D Targets for CO2 Capture from IGCC Power Plants*, in *Seventh Annual Conference on Carbon Capture & Sequestration*. 2008: Pittsburgh, PA.

8. Wong, S.B., *Carbon Dioxide Separation Technolgies*. 2002, Carbon & Energy Management, Alberta Research Council: Edmonton, Alberta.

9. Nenoff, T.M., R.J. Spontak, and C.M. Aberg, *Membranes for hydrogen purification: An important step toward a hydrogen-based economy.* Mrs Bulletin, 2006. **31**(10): p. 735-741.

10. Lin, H.Q., et al., *Plasticization-enhanced hydrogen purification using polymeric membranes.* Science, 2006. **311**(5761): p. 639-642.

11. Lin, H. and B.D. Freeman, *Gas solubility, diffusivity and permeability in poly(ethylene oxide).* Journal of Membrane Science, 2004. **239**(1): p. 105-117.

12. Reid, R.C., J.M. Prausnitz, and B.E. Poling, *The Properties of Gases and Liquids*. 4th ed. 1987, Boston: McGraw-hill. 752.

13. Robeson, L.M., *The upper bound revisited.* Journal of Membrane Science, 2008. **320**(1-2): p. 390-400.

14. Ritter, S.K., *What can we do with CO2.* Chemical and Engineering News, 2007. **85**(18): p. 7.

15. Franz, J. and V. Scherer, *An evaluation of CO2 and H2 selective polymeric membranes for CO2 separation in IGCC processes.* Journal of Membrane Science. **359**(1-2): p. 173-183.

16. Wu, G.X., C.L.B. Almquist, and S.T. Hwang, *High gas permeability in open-structure membranes.* Korean Journal of Chemical Engineering, 2004. **21**(2): p. 442-453.

17. Kim, K.H. and Y. Kim, *Theoretical Studies for Lewis Acid−Base Interactions and C−H···O Weak Hydrogen Bonding in Various CO_2 Complexes.* The Journal of Physical Chemistry A, 2008. **112**(7): p. 1596-1603.

18. Kilic, S., et al., *Effect of Grafted Lewis Base Groups on the Phase Behavior of Model Poly(dimethyl siloxanes) in CO2.* Industrial & Engineering Chemistry Research, 2003. **42**(25): p. 6415-6424.

19. Tapriyal, D., *Deepak's Proposal*. 2007, University of Pittsburgh. p. 49.

20. Donaldson, T.L. and Y.N. Nguyen, *Carbon Dioxide Reaction Kinetics and Transport in Aqueous Amine Membranes.* Industrial & Engineering Chemistry Fundamentals, 1980. **19**(3): p. 260-266.

21. Enick, R.M.B., Eric; Yazdi, Ali; Krukonis, Val; Schonemann, Hans; Howell, Jon, *Phase behavior of CO_2-perfluoropolyether oil mixtures and CO_2-perfluoropolyether chelating agent mixtures.* Journal of Supercritical Fluids, 1998. **13**.

22. O'Neill, M.L.C., Q.; Fang, M.; Johnson, K.P.; Wilkinson, S.P.; Smith, C.D.; Kerschner, J.L.; Jureller, S.H., *Solubility of Homopolymer and Copolymers in Carbon Dioxide.* Industrial & Engineering Chemistry Research, 1998. **37**(8): p. 3067-3079.

23. Bayraktar, Z.K., Erdogan, *Miscibility, phase separation, and volumetric properties of poly(dimethyl siloxane) in supercritical carbon dioxide.* Journal of Applied Polymer Science, 2000. **75**(11): p. 1397-1403.

24. Wohlfarth, C., ed. *CRC Handbook of Thermodynamic Data of Polymer Solutions at Elevated Pressures*. 2005, CRC Press: Boca Raton, FL.

25. Conway, S.E.B., H.-S; McHugh, M.A.; Wang, J.D.; Mandel, F.S., *Poly(lactide-co-glycolide) solution behavior in supercritical CO_2, CHF_3, and $CHClF_2$.* Journal of Applied Polymer Science, 2001. **80**(8): p. 1155-1161.

26. Kajiwara, M., *Gas permeability and selectivity of poly(organophosphazene) membranes.* Separation Science and Technology, 1991. **26**(6): p. 841-852.

27. Orme, C.J., et al., *Characterization of gas transport in selected rubbery amorphous polyphosphazene membranes.* Journal of Membrane Science, 2001. **186**(2): p. 249-256.

28. Nagai, K., et al., *Gas permeability of poly(bis-trifluoroethoxyphosphazene) and blends with adamantane amino/trifluoroethoxy (50/50).* Journal of Membrane Science, 2000. **172**(1): p. 167-176.

29. Kraus, M.A.M., Milton K. , *Polyphosphazene gas separation membranes*, ed. U.S.P.O. 4710204. Vol. 4710204, United States Patent No. 4710204 (1987).

30. Orme, C.J., et al., *Gas permeability in rubbery polyphosphazene membranes.* Journal of Membrane Science, 2006. **280**(1-2): p. 175-184.

31. Yin, Y., et al., *Synthesis and gas permeation properties of star-like poly(ethylene oxide)s using hyperbranched polyimide as central core.* Polymer Journal, 2004. **36**(4): p. 294-302.

32. Car, A., et al., *PEG modified poly(amide-b-ethylene oxide) membranes for CO2 separation.* Journal of Membrane Science, 2008. **307**(1): p. 88-95.

33. Patel, N.P., et al., *Tunable CO2 transport through mixed polyether membranes.* Journal of Membrane Science, 2005. **251**(1-2): p. 51-57.

34. Masuda, T., et al., *Diffusion and solution of gases in substituted polyacetylene membranes.* Polymer, 1988. **29**(11): p. 2041-2049.

35. Morisato, A. and I. Pinnau, *Synthesis and gas permeation properties of poly(4-methyl-2-pentyne).* Journal of Membrane Science, 1996. **121**(2): p. 243-250.

36. Simmons, J.W., *Block polyurethane-ether and polyurea-ether gas separation membranes*. L'Air Liquide-Societe Anonyme a'Directoire et Conseil de Surveillance pour l'Etude et l'Exploitation des Procedures Georges Claude (Paris, FR). Vol. 6843829, United States Patent No. 6843829 , (2005).

37. Yave, W., A. Car, and K.-V. Peinemann, *Nanostructured membrane material designed for carbon dioxide separation.* Journal of Membrane Science, 2010. **350**(1-2): p. 124-129.

38. Kazukiyo, N., H. Akon, and N. Tsutomu, *Gas permeability and stability of poly(1-trimethylsilyl-1-propyne-co-1-phenyl-1-propyne) membranes.* Journal of Polymer Science Part B: Polymer Physics, 1995. **33**(2): p. 289-298.

39. Bernardo, P., E. Drioli, and G. Golemme, *Membrane Gas Separation: A Review/State of the Art.* Industrial & Engineering Chemistry Research, 2009. **48**(10): p. 4638-4663.

40. Miller, M.B., et al., *Solubility of CO_2 in CO_2-philic oligomers; COSMOtherm predictions and experimental results.* Fluid Phase Equilibria, 2009. **287**(1): p. 26-32.

41. Shen, Z., et al., *CO2-solubility of oligomers and polymers that contain the carbonyl group.* Polymer, 2003. **44**(5): p. 1491-1498.

42. Wang, Y., et al., *Design and evaluation of nonfluorous CO_2-soluble oligomers and polymers.* Journal of Physical Chemistry B, 2009. **113**(45): p. 14971-14980.

43. *Carbon Dioxide Solubility Enhancement through Silicone Functionalization: CO2-philic Oligo(dimethylsiloxane)-substituted Diphosphonates*.* Separation Science and Technology, 2008. **43**: p. 2520-2536.

44. Stanley, R.S. and R.B. Florence, *Room temperature polymerization of glycidol.* Journal of Polymer Science Part A: Polymer Chemistry, 1966. **4**(5): p. 1253-1259.

45. Vandenberg, E.J., et al., *Poly(3-hydroxyoxetane) - an analog of poly(vinyl alcohol): Synthesis, characterization, and properties.* Journal of Polymer Science Part A: Polymer Chemistry, 1989. **27**(9): p. 3113-3149.

46. Blasig, A., et al., *Effect of Concentration and Degree of Saturation on RESS of a CO2-Soluble Fluoropolymer.* Industrial & Engineering Chemistry Research, 2002. **41**(20): p. 4976-4983.

47. Pinnau, I. and L.G. Toy, *Gas and vapor transport properties of amorphous perfluorinated copolymer membranes based on 2,2-bistrifluoromethyl-4,5-difluoro-1,3-dioxole/tetrafluoroethylene.* Journal of Membrane Science, 1996. **109**(1): p. 125-133.

48. Malucelli, G., et al., *Photopolymerization of poly(tetramethylene ether) glycol diacrylates and properties of the obtained networks.* Polymer, 1996. **37**(12): p. 2565-2571.

49. Damle, S. and W.J. Koros, *Permeation equipment for high-pressure gas separation membranes.* Industrial & Engineering Chemistry Research, 2003. **42**(25): p. 6389-6395.

50. Lugert, E.C., T.P. Lodge, and P. Bühlmann, *Plasticization of amorphous perfluoropolymers.* Journal of Polymer Science Part B: Polymer Physics, 2008. **46**(5): p. 516-525.

51. Pennline, H.W., et al., *Progress in carbon dioxide capture and separation research for gasification-based power generation point sources.* Fuel Processing Technology, 2008. **89**(9): p. 897-907.

52. Myers, C., et al., *High temperature separation of carbon dioxide/hydrogen mixtures using facilitated supported ionic liquid membranes.* Journal of Membrane Science, 2008. **322**(1): p. 28-31.

53. Millipore. *Stainless Steel Filter Holders*. [cited; Available from: http://www.millipore.com/catalogue/module/C263.

54. *Gas Sorption - PCTPro-2000*. [cited; Available from: http://www.setaram.com/PCTPro-2000.htm.

55. Muldoon, M.J., et al., *Improving Carbon Dioxide Solubility in Ionic Liquids.* The Journal of Physical Chemistry B, 2007. **111**(30): p. 9001-9009.

56. Bhide, B.D. and S.A. Stern, *Permeability of silicone polymers to hydrogen.* Journal of Applied Polymer Science, 1991. **42**(9): p. 2397-2403.

57. Alan, S.M. and J.B. Harris, *Flow of gases through polyethylene.* Journal of Polymer Science, 1961. **50**(154): p. 413-439.

58. Mehta, M. and M. Dole, *Hydrogen solubility in block copolymers of styrene and butadiene.* Macromolecules, 1982. **15**(2): p. 376-379.

59. Arnold, M.E., et al., *Gas permeation properties of poly(1,1 '-dihydroperfluorooctyl acrylate), poly(1,1 '-dihydroperfluorooetyl methacrylate), and poly(styrene)-b-poly(1,1 '-dihydroperfluorooctyl acrylate) block copolymers.* Macromolecules, 2001. **34**(16): p. 5611-5619.

60. Toi, K., Y. Maeda, and T. Tokuda, *Mechanism of diffusion and sorption of carbon dioxide in poly(vinyl acetate) above and below the glass transition temperature.* Journal of Membrane Science, 1983. **13**(1): p. 15-27.

61. Orme, C.J., et al., *Testing of polymer membranes for the selective permeability of hydrogen.* Separation Science and Technology, 2003. **38**(12): p. 3225 - 3238.

62. Lehermeier, H.J., J.R. Dorgan, and J.D. Way, *Gas permeation properties of poly(lactic acid).* Journal of Membrane Science, 2001. **190**(2): p. 243-251.

63. Komatsuka, T., A. Kusakabe, and K. Nagai, *Characterization and gas transport properties of poly(lactic acid) blend membranes.* Desalination, 2008. **234**(1-3): p. 212-220.

64. Lin, H., et al., *Transport and structural characteristics of crosslinked poly(ethylene oxide) rubbers.* Journal of Membrane Science, 2006. **276**(1): p. 145-161.

65. Brandrup, J.I., Edmund, H.; Grulke, Eric A.; Abe, Akihiro; Bloch, Daniel R., ed. *Polymer Handbook* 4th Edition ed. 1999, John Wiley & Sons: New York. 545-566.

66. Merkel, T.C., et al., *Gas sorption, diffusion, and permeation in poly(2,2-bis(trifluoromethyl)-4,5-difluoro-1,3-dioxole-co-tetrafluoroeth ylene).* Macromolecules, 1999. **32**(25): p. 8427-8440.

67. Langsam, M., M. Anand, and E.J. Karwacki, *Substituted propyne polymers : I. Chemical surface modification of poly[1-(trimethylsilyl] propyne] for gas separation membranes.* Gas Separation & Purification, 1988. **2**(4): p. 162-170.

68. Merkel, T.C., et al., *Mixed-gas permeation of syngas components in poly(dimethylsiloxane) and poly(1-trimethylsilyl-1-propyne) at elevated temperatures.* Journal of Membrane Science, 2001. **191**(1): p. 85-94.

69. Stropnik, C., et al., *Tailor-made Polymeric Membranes based on Segmented Block Copolymers for CO2 Separation.* Advanced Functional Materials, 2008. **18**(18): p. 2815-2823.

70. Patel, N.P., A.C. Miller, and R.J. Spontak, *Highly CO2-permeable and selective polymer nanocomposite membranes.* Advanced Materials, 2003. **15**(9): p. 729-733.

71. Wu, F., et al., *Transport study of pure and mixed gases through PDMS membrane.* Chemical Engineering Journal, 2006. **117**(1): p. 51-59.

72. Dlubek, G., F. Redmann, and R. Krause-Rehberg, *Humidity-induced plasticization and antiplasticization of polyamide 6: A positron lifetime study of the local free volume.* Journal of Applied Polymer Science, 2002. **84**(2): p. 244-255.

73. Scholes, C.A., G.W. Stevens, and S.E. Kentish, *The effect of hydrogen sulfide, carbon monoxide and water on the performance of a PDMS membrane in carbon dioxide/nitrogen separation.* Journal of Membrane Science. **350**(1-2): p. 189-199.

74. Yave, W., et al., *Gas permeability and free volume in poly(amide-b-ethylene oxide)/polyethylene glycol blend membranes.* Journal of Membrane Science, 2009. **339**(1-2): p. 177-183.

75. Jha, P., L.W. Mason, and J.D. Way, *Characterization of silicone rubber membrane materials at low temperature and low pressure conditions.* Journal of Membrane Science, 2006. **272**(1-2): p. 125-136.